HAL
open science

Viable Control of an Epidemiological Model

Michel de Lara, Lilian Sofia Sepulveda Salcedo

To cite this version:

Michel de Lara, Lilian Sofia Sepulveda Salcedo. Viable Control of an Epidemiological Model. Mathematical Biosciences, 2016, 280, pp.24-37. 10.1016/j.mbs.2016.07.010 . hal-01208484v2

HAL Id: hal-01208484

https://hal.science/hal-01208484v2

Submitted on 5 Jul 2019

HAL is a multi-disciplinary open access archive for the deposit and dissemination of scientific research documents, whether they are published or not. The documents may come from teaching and research institutions in France or abroad, or from public or private research centers.

L'archive ouverte pluridisciplinaire **HAL**, est destinée au dépôt et à la diffusion de documents scientifiques de niveau recherche, publiés ou non, émanant des établissements d'enseignement et de recherche français ou étrangers, des laboratoires publics ou privés.

Viable Control of an Epidemiological Model

Michel De Lara* Lilian Sofia Sepulveda Salcedo †

July 4, 2019

Abstract

In mathematical epidemiology, epidemic control often aims at driving the number of infected humans to zero, asymptotically. However, during the transitory phase, the number of infected individuals can peak at high values. Can we limit the number of infected humans at the peak? This is the question we address. More precisely, we consider a controlled version of the Ross-Macdonald epidemiological dynamical model: proportions of infected individuals and proportions of infected mosquitoes (vector) are state variables, and vector mortality is the control variable. We say that a state is viable if there exists at least one admissible control trajectory — time-dependent mosquito mortality rates bounded by control capacity — such that, starting from this state, the resulting proportion of infected individuals remains below a given infection cap for all times. The so-called viability kernel is the set of viable states. We obtain three different expressions of the viability kernel, depending on the couple control capacity-infection cap. In the comfortable case, the infection cap is high, the viability kernel is maximal and all admissible control trajectories are viable. In the desperate case, both control capacity and infection cap are too low and the viability kernel is the zero equilibrium without infection. In the remaining viable case, the viability kernel is neither zero nor maximal and not all admissible control trajectories are viable. We provide a numerical application in the case of the dengue outbreak in 2013 in Cali, Colombia.

*Université Paris-Est, Cermics (ENPC), F-77455 Marne-la-Vallée, delara@cermics.enpc.fr

†Universidad Autónoma de Occidente, Km. 3 vía Cali-Jamundí, Cali, Colombia, lssepulveda@uao.edu.co

Keywords: epidemiology; control theory; viability theory; Ross-Macdonald model; dengue.

1 Introduction

During the spread of an epidemic, the number of infected humans can peak at high values. Can we limit the number of infected individuals at the peak? This is the question we address. For an epidemic transmitted by mosquito vector and described by a Ross-Macdonald model, we study whether or not there exist trajectories of time-dependent vector mortality rates such that the number of infected individuals remains below a given infection cap for all times. This approach differs from the widespread stationary control strategies, based upon having control reproductive number stricly less than one to ensure convergence, and also from cost minimization optimal control ones.

Indeed, many studies on mathematical modeling of infectious diseases consist of analyzing the stability of the equilibria of a differential system (behavioral models such as SIR, SIS, SEIR [9]). Those studies focus on asymptotic behavior and stability, generally leaving aside the transient behavior of the system, where the infection can reach high levels. In many epidemiological models, a significant quantity is the "basic reproductive number" $\mathcal{R}_0$ which depends on parameters such as the transmission rate, the mortality and birth rate, etc. Numerous works (see references in [19, 14]) exhibit conditions on $\mathcal{R}_0$ such that the number of infected individuals tends towards zero. With this tool, different (time-stationary) management strategies of the propagation of the infection – quarantine, vaccination, etc. – are compared with respect to how they modify $\mathcal{R}_0$, that is, with respect to their capacity to drive the number of infected individuals towards zero, focusing on asymptotics. However, during the transitory phase, the number of infected can peak at high values.

Other works deal with the whole trajectory, as in dynamic optimization where strategies are compared with respect to intertemporal costs and benefits [20, 23, 18, 22, 12]. More recently, [17] studies controls that minimize the outbreak size (or infectious burden) under the assumption that there are limited control resources.

Our approach focuses both on transitories and asymptotics, in a robust way. Instead of aiming at an equilibrium or optimizing, we look for policies able to maintain the infected individuals below a threshold for all times.

To our knowledge, this approach is new in mathematical epidemiology. We have only found it mentioned in passing in [20] as a constraint – bounding above the maximum number infected at the peak – in a dynamic optimization problem, solved numerically.

In this paper, we formulate the problem as one of *viability*. In a nutshell, viability theory examines when and how can the state of a control system be maintained within a given region for all times [2]. Such problems of dynamic control under constraints also refer to invariance issues [10]. In the control theory literature, problems of constrained control lead to the study of positively invariant sets, particularly ellipsoidal and polyhedral ones for linear systems (see [5, 15, 16] and the survey paper [6]); reachability of target sets or tubes for nonlinear discrete time dynamics is examined in [4]. In continuous time, such a viability approach has been applied to models related to the sustainable management of fisheries [3], to viable strategies to ensure survival of some species [8], to secure the prey predator system [7], etc. In discrete-time, different examples can be found in [13] for sustainable management applications of viability.

The paper is organized as follows. In Section 2, we present a controlled version of the Ross-Macdonald dynamical model with two states — proportion of infected humans and proportion of infected mosquitoes — and with mortality control on the mosquito vector, by fumigation. Then we formulate the *viability problem* and introduce admissible control trajectories, that is, time-dependent mosquito mortality rates uniformly bounded by *control capacity*. We define the *viability kernel* as the set of initial states such that there exists at least one admissible mosquito mortality control trajectory that makes the resulting proportion of infected humans remain below a given *infection cap*, for all times. In Section 3, we provide three different expressions of the viability kernel, depending on the couple control capacity-infection cap. In the *comfortable case*, the infection cap is high, the viability kernel is maximal and all admissible control trajectories are viable. In the *desperate case*, both control capacity and infection cap are too low and the viability kernel is the zero equilibrium without infection. In the remaining *viable case*, the viability kernel is neither zero nor maximal and not all admissible control trajectories are viable. We also characterize *viable policies*. When the Ross-Macdonald model is driven by such policy — giving, at each time, a mosquito mortality rate as a function of current proportions of infected humans and mosquitoes — the proportion of infected humans remains

below the infection cap for all times. In Section 4, we provide a numerical application in the case of the dengue outbreak in 2013 in Cali, Colombia. Thanks to numerical data yielded by the Municipal Secretariat of Public Health of Cali, we can identify a Ross-Macdonald model, perform a viability analysis and point to practical applications of our work regarding mosquito control. We also lay out a sensitivity analysis for the viability kernel, displaying how it changes when the infection cap on the proportion of infected humans and the mosquito mortality maximal rate change. We conclude in Section 5. Some useful notions and results are collected in Section A in Appendix. Proofs are relegated in Section B. In Section C, we detail how we identify a Ross-Macdonald model thanks to numerical data provided by the Municipal Secretariat of Public Health of Cali.

2 The viability problem

First, we present the Ross-Macdonald model with control. Second, we formulate the viability problem — which consists in capping the proportion of infected humans yielded by the Ross-Macdonald dynamics — and we introduce the viability kernel.

2.1 The controlled Ross-Macdonald model

After introducing the Ross-Macdonald model, we turn it into a controlled dynamical system by adding a time-dependent vector mortality rate.

The Ross-Macdonald model

Different types of Ross-Macdonald models have been published [29]. We choose the one in [1], where both total populations (humans, mosquitoes) are normalized to 1 and divided between susceptibles and infected. The basic assumptions of the model are the following.

i) The human population (N_h) and the mosquito population (N_m) are closed and remain stationary.

ii) Humans and mosquitoes are homogeneous in terms of susceptibility, exposure and contact.

iii) The incubation period is ignored, in humans as in mosquitoes.

iv) Mortality induced by the disease is ignored, in humans as in mosquitoes.

v) Once infected, mosquitoes never recover.

vi) Only susceptibles get infected, in humans as in mosquitoes.

vii) Gradual immunity in humans is ignored.

Time is continuous, denoted by $t \in \mathbb{R}_+$. Let $m(t) \in [0,1]$ denote the *proportion of infected mosquitoes* at time t, and $h(t) \in [0,1]$ the *proportion of infected humans* at time t. Therefore, $1 - m(t)$ and $1 - h(t)$ are the respective proportions of susceptibles. The Ross-Macdonald model is the following differential system

$$\frac{dm}{dt} = \alpha p_m h(1-m) - \delta m \ , \tag{1a}$$

$$\frac{dh}{dt} = \alpha p_h \frac{N_m}{N_h} m(1-h) - \gamma h \ , \tag{1b}$$

where the parameters α, p_m, p_h, $\xi = \frac{N_m}{N_h}$, δ and γ are given in Table 1. The state space is the unit square $[0,1]^2$.

Parameter	Description	Unit
$\alpha \geq 0$	biting rate per time unit	time^{-1}
$\xi = N_m/N_h \geq 0$	number of female mosquitoes per human	dimensionless
$1 \geq p_h \geq 0$	probability of infection of a susceptible human by infected mosquito biting	dimensionless
$1 \geq p_m \geq 0$	probability of infection of a susceptible mosquito when biting an infected human	dimensionless
$\gamma \geq 0$	recovery rate for humans	time^{-1}
$\delta \geq 0$	(natural) mortality rate for mosquitoes	time^{-1}

Table 1: Parameters of the Ross-Macdonald model (1)

The controlled Ross-Macdonald model

For notational simplicity, we put

$$A_m = \alpha p_m \ , \ \ A_h = \alpha p_h \frac{N_m}{N_h} \ . \tag{2}$$

We turn the dynamical system (1) into a controlled system by replacing the natural mortality rate δ for mosquitoes in (1a) by a piecewise continuous function, called *control trajectory*

$$u(\cdot) : \mathbb{R}_+ \to \mathbb{R} \ , \ \ t \mapsto u(t) \ . \tag{3}$$

Therefore, the *controlled Ross-Macdonald model* is

$$\frac{dm}{dt} = A_m h(t)(1 - m(t)) - u(t)m(t) \ , \tag{4a}$$

$$\frac{dh}{dt} = A_h m(t)(1 - h(t)) - \gamma h(t) \ . \tag{4b}$$

For simplicity of notations (and for a more geometric approach to come in §3.3), with controlled system (4) we associate the controlled vector field (g_m, g_h) given by the two components

$$g_m(m, h, u) = A_m h(1 - m) - um \ , \tag{5a}$$

$$g_h(m, h) = A_h m(1 - h) - \gamma h \ . \tag{5b}$$

The controlled dynamical system (4) is equivalent to

$$\frac{dm}{dt} = g_m\big(m(t), h(t), u(t)\big) \ , \tag{6a}$$

$$\frac{dh}{dt} = g_h\big(m(t), h(t)\big) \ . \tag{6b}$$

2.2 The viability kernel

First, we lay out control constraints, then state constraints. With this, we formulate the viability problem and define the viability kernel.

Control capacity $\overline{u}$ and control constraints

Let $(\underline{u}, \overline{u})$ be a couple such that

$$\delta = \underline{u} < \overline{u} \ , \tag{7}$$

where δ is the natural mortality rate for mosquitoes (see Table 1). The parameter $\overline{u}$ is the *control capacity* or *mosquito mortality maximal rate*, a proxy for fumigation capacity.

We say that the control trajectory $u(\cdot)$ in (3) is *admissible* if it satisfies the *control constraints*

$$\underline{u} \leq u(t) \leq \overline{u} \ , \ \ \forall t \geq 0 \ . \tag{8}$$

As $\underline{u} = \delta$, the quantity $u(t) - \underline{u} \geq 0$ represents the fumigation mortality rate, additional to the natural mortality rate δ. The upper bound $\overline{u}$ is the maximal total mortality rate, that is, the natural mortality rate δ plus the fumigation mortality maximal rate. Thus, from now on, the function $u(\cdot)$ is the control on mosquito population that affects the mortality rate by fumigation of insecticides [26], in addition to the natural mortality rate.

Infection cap $\overline{H}$ and state constraints

Let $\overline{H}$ be a real number such that

$$0 < \overline{H} < 1 \ , \tag{9}$$

which represents the *maximum tolerated proportion of infected humans*, or *infection cap*. Thinking about public health policies set by governmental entities, we impose the following constraint: the proportion $h(t)$ of infected humans must always remain below the infection cap $\overline{H}$.

We say that the control trajectory $u(\cdot)$ in (3) is *viable* if it satisfies both the control constraints (8) (it is admissible) and if the state trajectory $\big(m(\cdot), h(\cdot)\big)$ solution of (4) satisfies the *state constraints*, called *viability constraints*,

$$h(t) \leq \overline{H} \ , \ \ \forall t \geq 0 \ . \tag{10}$$

The viability problem for the Ross-Macdonald model with control on the mosquito population is: when does there exist at least one viable control trajectory?

The viability kernel

The solution to the viability problem (3)-(4)-(8)-(10) is ultimately related to the initial conditions of infected mosquitoes and infected humans proportions.

Definition 1. *The* viability kernel *is the set of initial conditions* $(m_0, h_0) \in [0,1]^2$ *for which there exists at least one control trajectory* $u(\cdot)$ *as in* (3)*, satisfying the control constraints* (8) *and such that the solution to the controlled dynamical system* (4)*, with initial state* $\big(m(0), h(0)\big) = (m_0, h_0)$*, satisfies the state constraints* (10)*. We denote the viability kernel by*

$$\mathbb{V}(\overline{H}, \overline{u}) = \left\{ \begin{array}{c} (m_0, h_0) \\ \in [0,1]^2 \end{array} \middle| \begin{array}{c} \textit{there is a control trajectory } u(\cdot) \textit{as in } (3) \\ \textit{satisfying the control constraint } (8) \\ \textit{such that the solution } \big(m(\cdot), h(\cdot)\big) \textit{ to } (4) \\ \textit{which starts from } (m_0, h_0) \\ \textit{satisfies the state constraint } (10) \end{array} \right\} . \tag{11}$$

We will see the justification of the notation $\mathbb{V}(\overline{H}, \overline{u})$ in Theorem 2. Indeed, it will appear that $\mathbb{V}(\overline{H}, \overline{u})$ only depends on the infection cap $\overline{H}$ and on the control capacity $\overline{u}$ (and not on $\underline{u}$).

The viability kernel is a subset of the *constraint set*

$$\mathbb{V}^0(\overline{H}) = \{(m,h) | 0 \leq m \leq 1, 0 \leq h \leq \overline{H}\} = [0,1] \times [0, \overline{H}] \ , \tag{12}$$

that is,

$$\mathbb{V}(\overline{H}, \overline{u}) \subset \mathbb{V}^0(\overline{H}) \ . \tag{13}$$

3 Characterization of the viability kernel

In this section, we will state our main result, the characterization of the viability kernel $\mathbb{V}(\overline{H}, \overline{u})$ in (11) depending on the couple control capacity $\overline{u}$ and infection cap $\overline{H}$. Then, we will discuss the epidemiological interpretation and characterize so-called viable policies.

3.1 Main result

The following theorem describes the viability kernel $\mathbb{V}(\overline{H}, \overline{u})$ depending on the couple control capacity $\overline{u}$ and infection cap $\overline{H}$. In the *comfortable case*, the infection cap is high, the viability kernel is maximal and all admissible control trajectories are viable. In the *desperate case*, both control capacity and infection cap are too low and the viability kernel is the zero equilibrium without infection. In the remaining *viable case*, the viability kernel is neither

zero nor maximal and not all admissible control trajectories are viable. The proof of Theorem 2 is given in Section B in Appendix.

Theorem 2. *The viability kernel* $\mathbb{V}(\overline{H}, \overline{u})$ *in* (11) *is as follows.*[1]

C) *Comfortable case: if*

$$\overline{H} \geq \frac{A_h}{A_h + \gamma} \ , \tag{14}$$

the viability kernel $\mathbb{V}(\overline{H}, \overline{u})$ *is the whole constraint set* $\mathbb{V}^0(\overline{H})$ *in* (12), *that is,*

$$\mathbb{V}(\overline{H}, \overline{u}) = [0, 1] \times [0, \overline{H}] \ . \tag{15}$$

D) *Desperate case: if*

$$A_m(A_h + \gamma)\overline{H} + \gamma\overline{u} < A_m A_h \ , \tag{16}$$

the viability kernel consists only of the origin (equilibrium without infection):

$$\mathbb{V}(\overline{H}, \overline{u}) = \{(0, 0)\} \ . \tag{17}$$

V) *Viable case: if*

$$\overline{H} < \frac{A_h}{A_h + \gamma} \ , \tag{18a}$$

$$A_m(A_h + \gamma)\overline{H} + \gamma\overline{u} > A_m A_h \ , \tag{18b}$$

the viability kernel $\mathbb{V}(\overline{H}, \overline{u})$ *is a strict subset of the constraint set* $\mathbb{V}^0(\overline{H})$, *with the following expression*

$$\begin{aligned} \mathbb{V}(\overline{H}, \overline{u}) =& [0, \overline{M}] \times [0, \overline{H}] \\ & \bigcup \left\{ (m, h) \middle| \overline{M} \leq m \leq M_\infty \ , \ \ h \leq \mathcal{H}(m) \right\} \ . \end{aligned} \tag{19}$$

In this expression, we have

$$\overline{M} = \frac{\gamma\overline{H}}{A_h(1 - \overline{H})} \ , \ \ 0 < \overline{M} < 1 \ , \tag{20}$$

[1]Notice that we do not study the case $A_m(A_h + \gamma)\overline{H} + \gamma\overline{u} = A_m A_h$ (see Footnote 2).

and the upper right frontier of the viability kernel $\mathbb{V}(\overline{H}, \overline{u})$ *is a smooth and decreasing curve parameterized by* $\mathcal{H} : [\overline{M}, M_\infty] \to [0, \overline{H}]$*, solution of the differential equation*

$$-g_m(m, \mathcal{H}(m), \overline{u})\mathcal{H}'(m) + g_h(m, \mathcal{H}(m)) = 0 \ , \tag{21a}$$

$$\mathcal{H}(\overline{M}) = \overline{H} \ , \tag{21b}$$

with $M_\infty > \overline{M}$ *such that*

$$\textit{either} \quad \overline{M} < M_\infty < 1 \qquad \textit{and } \mathcal{H}(M_\infty) = 0 \ , \tag{21c}$$

$$\textit{or} \quad M_\infty = 1 \qquad \textit{and } \mathcal{H}(M_\infty) > 0 \ . \tag{21d}$$

Examples of viability kernels in the viable case V) are shown on Figures 2 (case (21c)) and 3 (case (21d)).

On Figure 1, we visualize how the viability kernel $\mathbb{V}(\overline{H}, \overline{u})$ varies with the infection cap $\overline{H}$ and the mosquito mortality maximal rate $\overline{u}$.

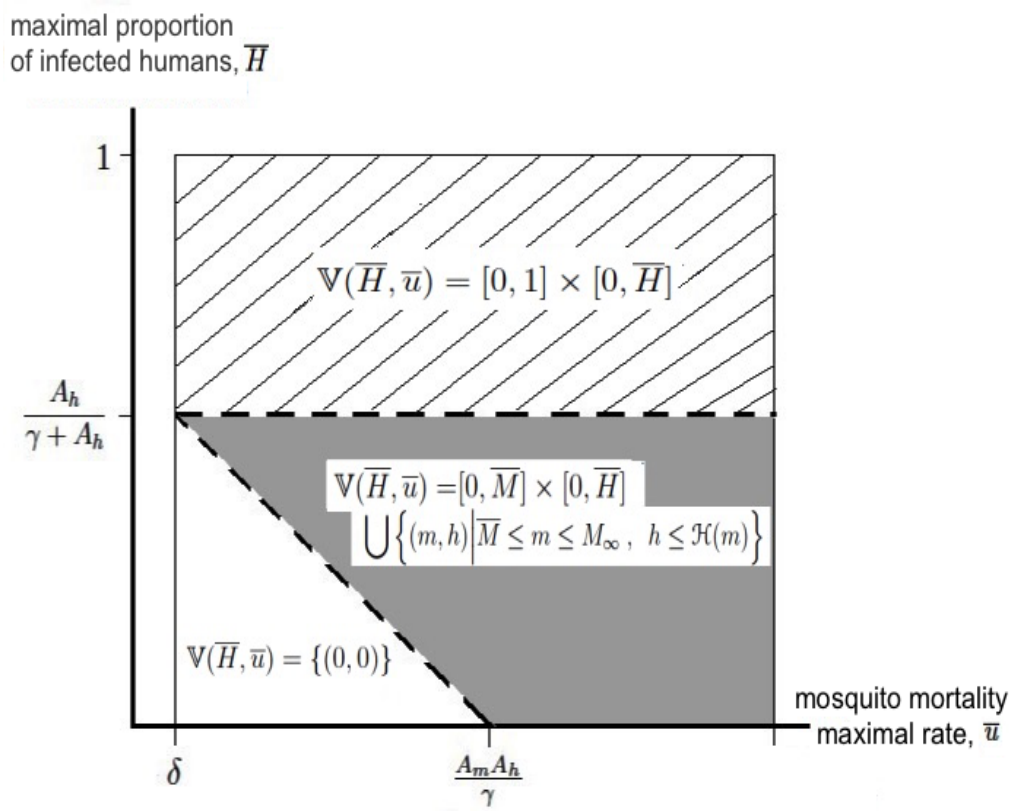

Figure 1: Three cases for the viability kernel for the controlled Ross-Macdonald model (4), in function of the infection cap $\overline{H}$ on the proportion of infected humans and of the mosquito mortality maximal rate $\overline{u}$

Equalities in the inequalities (18a) and (18b) correspond to the two dashed straight lines on Figure 1.

C) When the couple $(\overline{u}, \overline{H})$ belongs to the upper rectangle shaded with lines (corresponding to a high infection cap $\overline{H}$), the viability kernel is the whole constraint set $\mathbb{V}^0(\overline{H}) = [0,1] \times [0, \overline{H}]$.

D) When the couple $(\overline{u}, \overline{H})$ belongs to the unshaded bottom triangle, the viability kernel consists only of the origin.

V) When the couple $(\overline{u}, \overline{H})$ belongs to the the gray shaded region, the viability kernel is a strict subset of the constraint set $\mathbb{V}^0(\overline{H}) = [0,1] \times [0, \overline{H}]$,

whose top right frontier is the smooth curve given in (21a)–(21b).

3.2 Epidemiological interpretation

The results of Theorem 2 make sense from an epidemiological point of view.

C) One extreme situation is when the infection cap $\overline{H}$ on the proportion of infected humans is high. In that case, we are allowing a large fraction of the population to get infected. For any initial state in the so-called constraint set (that is, such that the value with which the proportion of people starts is located below the infection cap $\overline{H}$), there are viable trajectories of mosquito mortality rates — admissible and that make the proportion of infected humans always below infection cap $\overline{H}$ for all times. In fact, we will see in §3.3 that any admissible control trajectory is viable.

D) The other extreme situation is when both the infection cap $\overline{H}$ and the control capacity $\overline{u}$ are low, in the sense that they satisfy (16). In that case, the imposed constraints — the state constraints (10) that the proportion of infected humans does not overshoot $\overline{H}$ and the control constraints (8) that the mosquito mortality rate cannot exceed $\overline{u}$ — can only be satisfied when there are no infected humans nor infected mosquitoes at the start. For any other initial state, even the mosquito mortality maximal rate $\overline{u}$ is not sufficient to prevent the infected mosquitoes from reaching levels where they will induce a proportion of infected humans above the infection cap $\overline{H}$.

V) The most interesting case is when the infection cap $\overline{H}$ is not too high as in (18a) and that, with the mosquito mortality maximal rate $\overline{u}$, they jointly satisfy (18b). Indeed, when the control constraints (8) and the state constraints (10) are medium — that is, not too weak or too strong — the viability kernel $\mathbb{V}(\overline{H}, \overline{u})$ is in-between the origin $\{(0,0)\}$ and the entire constraint set $\mathbb{V}^0(\overline{H})$ in (12). In that case, there are viable trajectories of mosquito mortality rates — admissible and that make the proportion of infected humans always below the infection cap $\overline{H}$ for all times — but only for initial states inside the viability kernel. Figures 2 and 3 provide two illustrations of viability kernels. The viability kernel is the strict subset (19) of the constraint set $\mathbb{V}^0(\overline{H})$. It is made of two subsets as follows.

- When the proportion m of infected mosquitoes is low, namely less than $\overline{M}$ in (20), any initial condition $\big(m, h\big)$ is viable as soon as $h \leq \overline{H}$. Notice that $\overline{M}$ is the proportion m of infected mosquitoes such that, on the line $h = \overline{H}$, the component $g_h(m, h)$ in (5b) is zero, that is

$$g_h(\overline{M}, \overline{H}) = A_h \overline{M}(1 - \overline{H}) - \gamma \overline{H} = 0 \ . \tag{22}$$

- When the proportion m of infected mosquitoes is high, namely more than $\overline{M}$ in (20), it is not sufficient that $h \leq \overline{H}$ for the initial condition $\big(m, h\big)$ to be viable. To be viable, the state $\big(m, h\big)$ has to be below the top right frontier delineated by the smooth curve given in (21a)–(21b). This upper frontier matches the state orbit associated with the mosquito mortality maximal rate $\overline{u}$ (as proved in Lemma 17). Two typical shapes for the top right frontier can be seen on Figures 2 and 3.
  - Figure 2. In the case (21c) where $\overline{M} < M_\infty < 1$ and $\mathcal{H}(M_\infty) = 0$, the infection cap $\overline{H}$ is so low that initial states with high proportion m of infected mosquitoes, namely more than M_∞, are not viable.
  - Figure 3. In the case (21d) where $M_\infty = 1$ and $\mathcal{H}(M_\infty) > 0$, there are initial states with proportion m of infected mosquitoes up to 100%.

3.3 Viable policies

After having characterized the viability kernel, we now turn to discuss so-called *viable policies*.

In practice, viable control trajectories (as defined in §2.2) are produced by viable policies. An *admissible policy* is a state feedback

$$\widehat{U}_m : [0, 1]^2 \to [\underline{u}, \overline{u}] \ . \tag{23}$$

A *viable policy* is an admissible policy such that the solution to the controlled dynamical system (4), driven by the control trajectory $u(\cdot)$ given by

$$u(t) = \widehat{U}_m\big(m(t), h(t)\big) \ , \ \ \forall t \geq 0 \ , \tag{24}$$

satisfies the state constraints (10), for any initial state $\big(m(0), h(0)\big) = (m_0, h_0)$ in the viability kernel $\mathbb{V}(\overline{H}, \overline{u})$. Notice that, by imposing in (23) that the policy $\widehat{U}_m$ takes value in $[\underline{u}, \overline{u}]$, the control constraints (8) are satisfied.

Viable policies can be obtained from geometric considerations. In viability theory [2], it is proven that any control $u \in [\underline{u}, \overline{u}]$, such that the vector (g_m, g_h) in (5) points towards the inside of the viability kernel $\mathbb{V}(\overline{H}, \overline{u})$ induces a viable policy. With this latter, any initial state in $\mathbb{V}(\overline{H}, \overline{u})$ produces a state trajectory in $\mathbb{V}(\overline{H}, \overline{u})$.

C) In the comfortable case — with a high infection cap $\overline{H}$ as in (14) — the state constraints (10) are weak, and the constraint set $\mathbb{V}^0(\overline{H}) = [0, 1] \times [0, \overline{H}]$ is strongly invariant by Proposition 13. Therefore, *any* admissible control trajectory makes it possible that the proportion of infected humans remains below the infection cap $\overline{H}$ for all times. For instance, the constant policy $\widehat{U}_m : (m, h) \mapsto \underline{u} = \delta$ — corresponding to natural mortality rate (hence to no control) — is a viable policy, that induces the stationary control trajectory $u(\cdot) \equiv \underline{u}$.

D) In the desperate case — when both the infection cap $\overline{H}$ and the control capacity $\overline{u}$ are low, in the sense that they satisfy (16) — it is impossible to keep the proportion of infected humans below the infection cap $\overline{H}$ for all times, for *whatever* admissible control trajectory, except if there are no infected humans or mosquitoes at the start, by Proposition 14.

V) In the viable case, a viable policy is the constant policy $\widehat{U}_m : (m, h) \mapsto \overline{u}$ — corresponding to maximal fumigation — that induces the stationary control trajectory $u(\cdot) \equiv \overline{u}$. However, there are other viable policies, less "costly" in terms of fumigation effort. Indeed, to be viable, it suffices that, on the frontier of the viability kernel $\mathbb{V}(\overline{H}, \overline{u})$, a policy yields a vector (g_m, g_h) in (5) that points towards the inside of $\mathbb{V}(\overline{H}, \overline{u})$. For instance, we could opt for a policy — defined only inside the viability kernel $\mathbb{V}(\overline{H}, \overline{u})$ — which gives to the control values close to $\underline{u}$ when far from the frontier of the viability kernel $\mathbb{V}(\overline{H}, \overline{u})$, but reaches $\overline{u}$ when close to the frontier.

4 Numerical application in the case of the dengue outbreak in 2013 in Cali, Colombia

Thanks to numerical data yielded by the Municipal Secretariat of Public Health of Cali, we have identified, in Section C, parameters of the Ross-Macdonald model in (72a) and estimates for the range of mosquito mortality rates in (72b)-(72c). With this material, we first perform a viability analysis in the case of the dengue outbreak in 2013 in Cali, Colombia. Second, we lay out a sensitivity analysis for the viability kernel, displaying how it changes when the infection cap $\overline{H}$ on the proportion of infected humans and the mosquito mortality maximal rate $\overline{u}$ change.

4.1 Viability analysis

Here, we consider the results of Theorem 2 with data from Section C. What our analysis suggests is the following.

C) When the infection cap $\overline{H}$ on the proportion of infected humans is high (comfortable case), here when $\overline{H} \geq \frac{A_h}{A_h+\gamma} \approx 42\%$ (quite a high proportion), then any admissible policy will ensure that the state constraints (10) be satisfied, as long as the initial number of infected individuals is below the infection cap $\overline{H}$.

D) The desperate case occurs when the condition $0.013 \times \overline{H} + 0.1 \times \overline{u} < 0.005$ is met. As $\overline{H} > 0$, the desperate case cannot occur when the fumigation capacity is so high that $\overline{u} > 0.005/0.1 = 0.055$ day^{-1} (see Figure 1). By contrast, for the desperate case to occur, the infection cap $\overline{H}$ has necessarily to be low; indeed, as $\overline{u} > \underline{u} = \delta = 0.0333$ day^{-1}, we must have that $\overline{H} < 17\%$.

V) The viable case occurs when $\overline{H} < 42\%$ and $0.013 \times \overline{H} + 0.1 \times \overline{u} > 0.005$. We now detail two subcases, focusing on viable policies.

Case $\overline{u} = 0.05$ day^{-1} and $\overline{H} = 1\%$

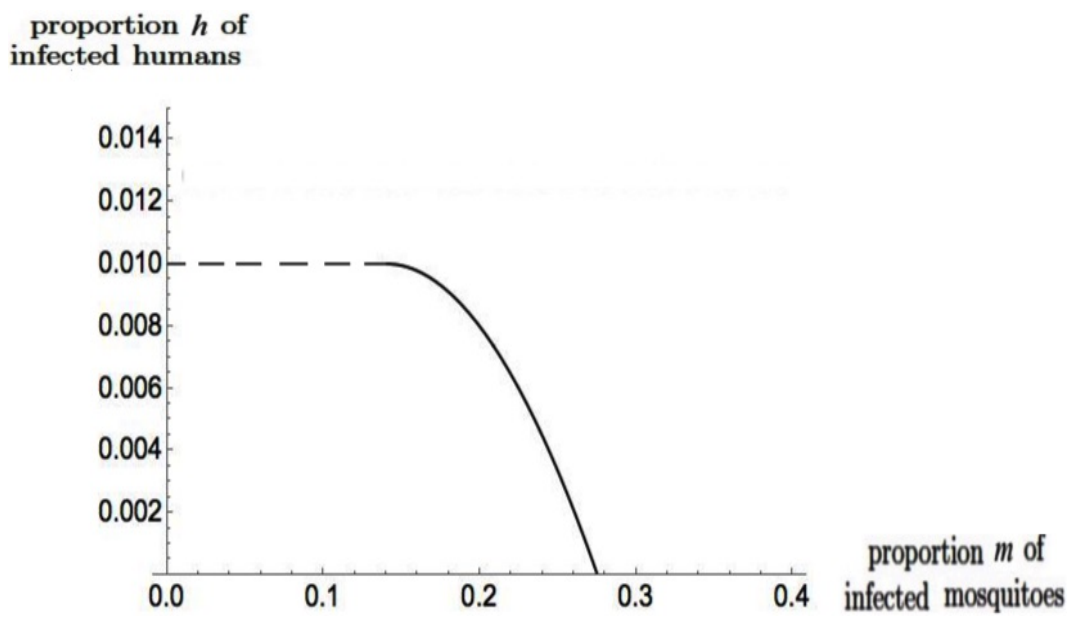

Figure 2: Case (48b) with $M_\infty < 1$ and $\mathcal{H}(M_\infty) = 0$. Solution graph for the differential equation (21a)–(21b), with parameters (72a) (adjusted to the 2013 dengue outbreak in Cali, Colombia), and with $\overline{u} = 0.05$ day^{-1} and $\overline{H} = 1\%$

The viability kernel $\mathbb{V}(\overline{H}, \overline{u})$ for $\overline{u} = 0.05$ day^{-1} and $\overline{H} = 1\%$ is displayed in Figure 2. By (20), we have

$$\overline{M} = 14\% \ . \tag{25}$$

The numerical solution $\mathcal{H}$ of the differential equation (21a)–(21b) has the property to take the value 0. We are in the case (21c) and we obtain

$$M_\infty = 27\% \quad \text{and} \quad \mathcal{H}(M_\infty) = 0 \ . \tag{26}$$

Here, the infection cap $\overline{H} = 1\%$ is so low that initial states with high proportion m of infected mosquitoes, namely more than M_∞, are not viable. The numbers $\overline{M} = 14\%$ and $M_\infty = 27\%$, together with Figure 2, have practical implications for the viable control of dengue. What the analysis in §3.3 suggests is that, to cap the proportion of infected humans at the peak, you

need to measure the proportion of infected mosquitoes. Measuring mosquito abundance is a difficult task, whereas measuring a *proportion* of infected mosquitoes might be done by proper sampling. Here is a possible design for a viable policy.

- *Monitoring without fumigation.* When the proportion of infected humans is below the infection cap $\overline{H} = 1\%$ and when the proportion of infected mosquitoes is below the proportion $\overline{M} = 14\%$, do not fumigate.

- *Monitoring with (maximal) fumigation.* When the proportion of infected mosquitoes is between the proportions $\overline{M} = 14\%$ and $M_\infty = 27\%$, fumigate with maximal capacity.

- *Alert.* When the proportion of infected mosquitoes is above $M_\infty = 27\%$, additional measures should be taken to prevent a high peak of infected humans.

Case $\overline{u} = 0.04$ day^{-1} and $\overline{H} = 5\%$

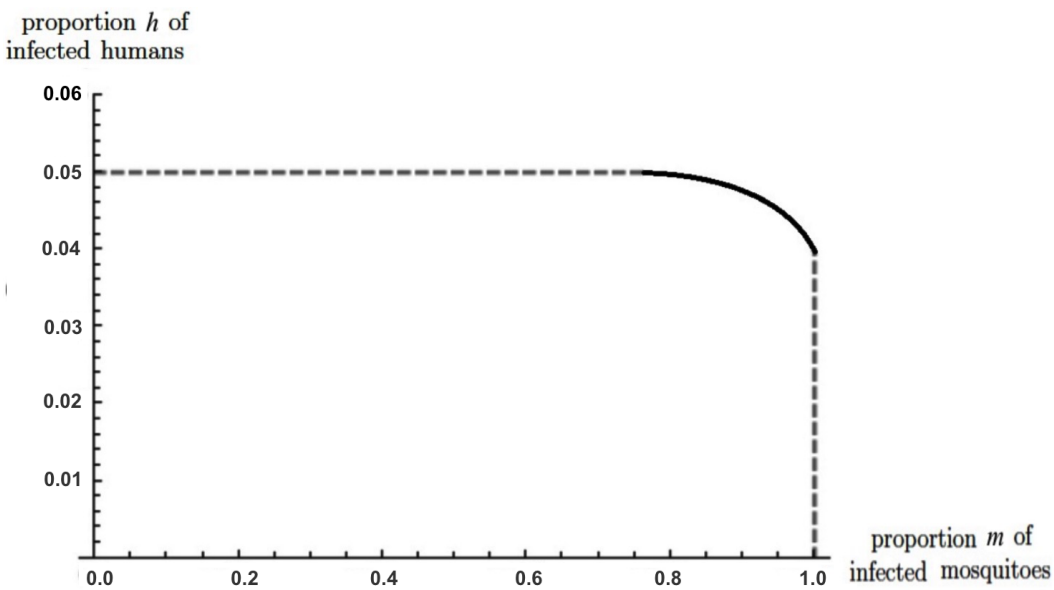

Figure 3: Case (21d) with $M_\infty = 1$ and $\mathcal{H}(M_\infty) > 0$. Solution graph for the differential equation (21a)–(21b), with parameters (72a) (adjusted to the 2013 dengue outbreak in Cali, Colombia), and with $\overline{u} = 0.04$ day^{-1} and $\overline{H} = 5\%$

The viability kernel $\mathbb{V}(\overline{H}, \overline{u})$ for $\overline{u} = 0.04$ day^{-1} and $\overline{H} = 5\%$ is displayed in Figure 3. Here, we obtain

$$\overline{M} = 73\% \quad \text{and} \quad M_\infty = 100\% \,. \tag{27}$$

These numbers, together with Figure 2, can also suggest possible designs for viable dengue control. We do not detail this case because $\overline{H} = 5\%$ is a high and irrealistic infection cap.

4.2 Sensitivity analysis for the viability kernel

Here, we present figures displaying how the viability kernel $\mathbb{V}(\overline{H}, \overline{u})$ changes when the infection cap $\overline{H}$ on the proportion of infected humans and the

mosquito mortality maximal rate $\overline{u}$ change. We restrict the sensitivity analysis to the viable case V), the only interesting case because, in the two other cases, the viability kernel does not change (see Theorem 2).

Sensitivity of $\mathbb{V}(\overline{H}, \overline{u})$ with respect to the infection cap $\overline{H}$ on the proportion of infected humans

On Figure 4, we display two viability kernels (when the mosquito mortality maximal rate $\overline{u} = 0.05$ day^{-1}) corresponding to two values — 1% and 5% — for the infection cap $\overline{H}$ on the proportion of infected humans. Quite naturally, as $\overline{H}$ increases, the state constraints (10) are easier to satisfy, so that the viability kernel $\mathbb{V}(\overline{H}, \overline{u})$ increases too.

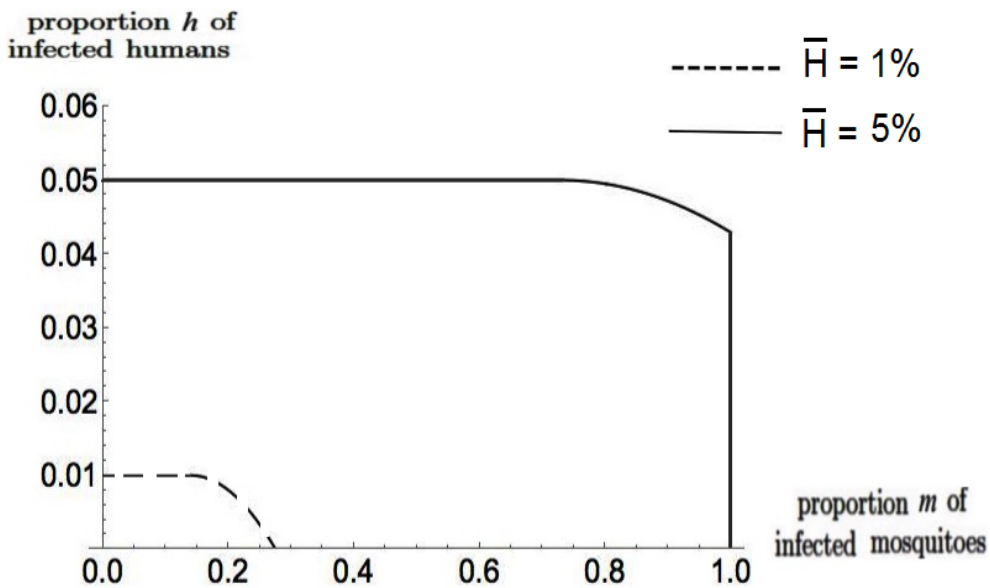

Figure 4: Examples of viability kernels for the controlled Ross-Macdonald model (4), corresponding to two values — 1% and 5% — for the infection cap $\overline{H}$ on the proportion of infected humans, for mosquito mortality maximal rate $\overline{u} = 0.05$ day^{-1}. Parameters are adjusted to the 2013 dengue outbreak in Cali, Colombia

Sensitivity of $\mathbb{V}(\overline{H}, \overline{u})$ with respect to the mosquito mortality maximal rate $\overline{u}$

On Figure 5, we display two viability kernels (when the infection cap $\overline{H} = 1\%$) corresponding to two values — 0.035 day^{-1} and 0.05 day^{-1} — for the mosquito mortality maximal rate $\overline{u}$. Quite naturally, as $\overline{u}$ increases, the set of admissible control trajectories — those $u(\cdot)$ as in (3) that satisfy the control constraints (8) — is enlarged, so that the viability kernel $\mathbb{V}(\overline{H}, \overline{u})$ increases too.

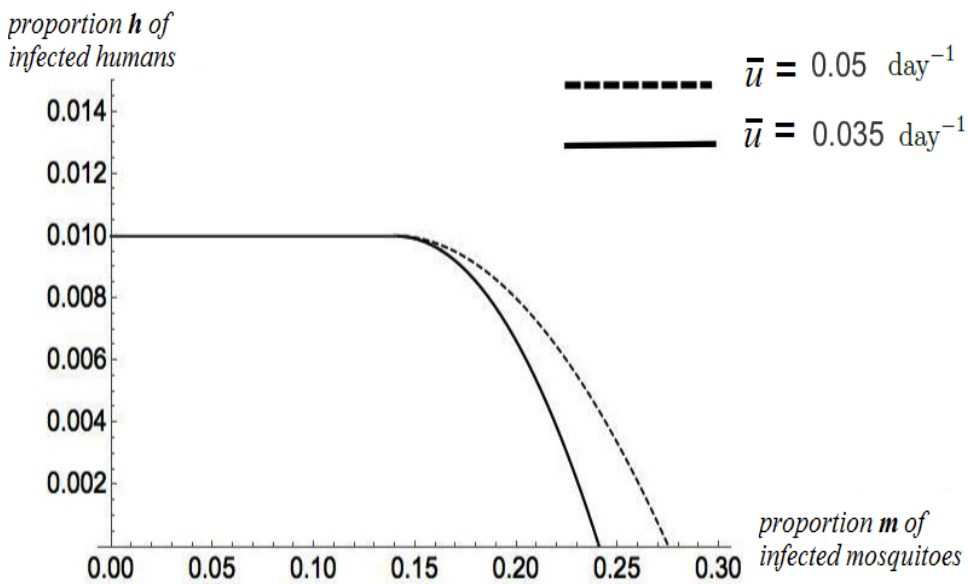

Figure 5: Examples of viability kernels for the controlled Ross-Macdonald model (4), corresponding to two values — 0.035 day^{-1} and 0.05 day^{-1} — for the mosquito mortality maximal rate $\overline{u}$, for infection cap $\overline{H} = 1\%$. Parameters are adjusted to the 2013 dengue outbreak in Cali, Colombia

5 Conclusion

As said in the introduction, the approach we have developed is (to our best knowledge) new in mathematical epidemiology. Instead of aiming at an equilibrium or optimizing, we have looked for policies able to maintain the infected individuals below a threshold for all times. More precisely, we have allowed for time-dependent mosquito mortality rates to reduce the population

of mosquito vector, in order to maintain the proportion of infected individuals by dengue below a cap for all times. By definition, the viability kernel is the set of initial states (infected mosquitoes and infected individuals) for which such a mosquito mortality control trajectory exists.

Our theoretical results are the following. For the Ross-Macdonald model with vector mortality control, we have been able to characterize the viability kernel associated with the viability constraint that consists in capping the proportion of infected humans for all times. We have provided three expressions of the viability kernel depending on the relative values of, on the one hand, the cap on the proportion of infected individuals, and of, on the other hand, the mosquito mortality maximal rate (a proxy for the fumigation capacity). We have also characterized so-called viable policies that produce, at each time, a mosquito mortality rate as a function of current proportions of infected humans and mosquitoes, such that the proportion of infected humans remains below the infection cap for all times. Regarding the use of our theoretical results, we have provided a numerical application in the case of the dengue outbreak in 2013 in Cali, Colombia.

What our analysis suggests is that, to cap the proportion of infected humans at the peak, you need in addition to measure the proportion of infected mosquitoes, at least when it is larger than the characteristic proportion $\overline{M}$, defined in (20). Measuring mosquito abundance is a difficult task, whereas measuring a *proportion* of infected mosquitoes might be done by proper sampling. Naturally, the weaker the control capacity, the more you need to estimate the proportion of infected mosquitoes, as illustrated in Figure 5.

A Appendix. Viable equilibria, viability domains and monotonicity properties

We introduce notions and properties that will prove useful in the proofs in Section B.

A.1 Viable equilibria

Controlled systems display a family of equilibria, indexed by stationary control trajectories. Within them, the equilibria which satisfy the state and

control constraints are part of the viability kernel: they are said to be *viable equilibria.*

Definition 3. *A* stationary control trajectory *is a control trajectory* $u(\cdot)$ *as in* (3)*, such that*

$$u(t) = u^e \ , \ \ \forall t \geq 0 \ , \quad \textit{with } \underline{u} \leq u^e \leq \overline{u} \ . \tag{28}$$

The viable equilibria *of the controlled dynamical system* (4) *are the equilibria of the system* (4) *with stationary control trajectories.*

To describe viable equilibria, we introduce the condition

$$\underline{u} \leq u^e \leq \overline{u} \quad \text{and} \quad \frac{A_m A_h}{\gamma} - \frac{A_m(A_h+\gamma)}{\gamma}\overline{H} \leq u^e < \frac{A_m A_h}{\gamma} \ , \tag{29}$$

or, equivalently, the condition

$$\underline{u} \leq u^e \leq \overline{u} \quad \text{and} \quad u^e < \frac{A_m A_h}{\gamma} \quad \text{and} \quad \frac{A_h - \gamma u^e/A_m}{A_h+\gamma} \leq \overline{H} \ . \tag{30}$$

Proposition 4.

- *When* (29)*, or* (30)*, does not holds true, the disease free equilibrium* $(0,0)$ *is the only viable equilibrium of the controlled system* (4) *with control* $u(\cdot) \equiv u^e$*. In addition, the disease free equilibrium* $(0,0)$ *is globally asymptotically stable.*

- *When* (29)*, or* (30)*, holds true, the disease free equilibrium* $(0,0)$ *and the endemic equilibrium point*

$$(m^e, h^e) = \left(\frac{A_m - \gamma u^e/A_h}{A_m + u^e}, \frac{A_h - \gamma u^e/A_m}{A_h+\gamma} \right) \tag{31}$$

  are the only viable equilibria of the controlled system (4) *with control* $u(\cdot) \equiv u^e$*. In addition, the endemic equilibrium points* (31) *are globally asymptotically stable.*

Proof. Consider stationary mosquito control, that is, constant mortality rate as in (28). The system (4)–(28) has the disease free equilibrium $(0,0)$ and,

possibly, the endemic equilibrium point (31). Such point (m^e, h^e) exists in $[0,1]^2$ and is different from $(0,0)$ when

$$\underline{u} \leq u^e \leq \overline{u} \quad \text{and} \quad 0 < A_m A_h - \gamma u^e \ . \tag{32}$$

The viable equilibria are those states (m^e, h^e) for which both (32) and $h^e \leq \overline{H}$ hold true. The condition $h^e \leq \overline{H}$ is equivalent to $\frac{A_h - \gamma u^e / A_m}{A_h + \gamma} \leq \overline{H}$. Rearranging the expressions in (32), we obtain (29) and (30).

The proof that the viable equilibria (31) or the disease free equilibrium $(0,0)$ are globally asymptotically stable is classical. It relies on the Poincaré-Bendixson theorem, excluding periodic orbits thanks to the Bendixson-Dulac criterion [31]. □

A.2 Viability domains

We define and present a geometric characterization of so-called viability domains of the controlled dynamical system (4), as they will be an important step to characterize the viability kernel.

Definition 5. *A subset $\mathbb{V}$ of the state space $[0,1]^2$ is said to be a* viability domain *for the controlled dynamical system* (4)*, with the control constraints* (8)*, if there exists an admissible control trajectory $u(\cdot)$ such that the solution to* (4)*, which starts from $\big(m(0), h(0)\big) \in \mathbb{V}$, remains within $\mathbb{V}$ for every $t \geq 0$.*

Viability domains are related to the viability kernel as follows.

Theorem 6 ([2])**.** *The viability kernel $\mathbb{V}(\overline{H}, \overline{u})$ in* (11) *is the largest viability domain within the constraint set $\mathbb{V}^0(\overline{H})$ in* (12)*.*

We now provide a geometric characterization of the viability domains of the controlled dynamical system (6), with the control constraints (8), using the controlled vector field (g_m, g_h) in (5). For this purpose, we first note that the controlled dynamical system (6) is *Marchaud* [2] because:

- the constraints (8) on the controls are written as $u \in [\underline{u}, \overline{u}]$, where $[\underline{u}, \overline{u}]$ is closed;
- the components of the controlled vector field (g_m, g_h) in (5) are continuous;

- the controlled vector field (g_m, g_h) and the set $[\underline{u}, \overline{u}]$ have linear growth, because the partial derivatives of (g_m, g_h) (with respect to the state variables) are smooth and defined over the compact $[0,1]^2$;
- the set $\{(g_m, g_h)(m, h, u) \mid u \in [\underline{u}, \overline{u}]\}$ is convex, for all (m, h), because $g_m(m, h, u)$ is linearly dependent on the control u.

Second, we will use the following result to be found in [2] (Theorem 6.1.4, p. 203 and the remark p. 200).

Proposition 7. *For a Marchaud controlled dynamical system, a closed subset $\mathbb{V}$ is viable if the tangent cone at any point in $\mathbb{V}$ contains at least one of the vectors in the family generated by the controlled vector field at this point when the control varies.*

In our case, we obtain the following geometric characterization of viability domains.

Proposition 8. *Consider a closed subset $\mathbb{V}$ of $[0,1]^2$. The set $\mathbb{V}$ is a viability domain for the controlled dynamical system* (4)*, with the control constraints* (8)*, if, whenever (m, h) varies along the frontier $\partial\mathbb{V}$ of the set $\mathbb{V}$, there is a control $u \in [\underline{u}, \overline{u}]$ such that $(g_m(m, h, u), g_h(m, h))$ in* (5) *is an inward-pointing vector, with respect to the set $\mathbb{V}$.*

If the closed subset $\mathbb{V}$ has a piecewise smooth frontier $\partial\mathbb{V}$, it suffices — for the set $\mathbb{V}$ to be a viability domain for the controlled dynamical system (4), with the control constraints (8) — that the scalar product between the vector (g_m, g_h) in (5) and a normal (non zero) outward-pointing vector (with respect to the set $\mathbb{V}$) be less than or equal to zero.

A.3 Monotonicity properties

The controlled dynamical system (4) has monotonicity properties which will be practical for characterizing the viability kernel.

Proposition 9. *Let $\big(m(\cdot), h(\cdot)\big)$ be the solution to* (4) *for an admissible control trajectory $u(\cdot)$. Let $\big(\overline{m}(\cdot), \overline{h}(\cdot)\big)$ be the solution to* (4) *for the stationary admissible control trajectory $u(\cdot) \equiv \overline{u}$. If*

$$\overline{m}(0) \leq m(0) \ , \ \ \overline{h}(0) \leq h(0) \ , \tag{33}$$

we have that

$$\overline{m}(t) \leq m(t) \ , \ \ \overline{h}(t) \leq h(t) \ , \ \ \forall t \geq 0 \ . \tag{34}$$

Proof. To prove the result, we will make use of the Definition 10 of quasi monotonous vector fields, and of the comparison Theorem 12, to be found right after the proof.

For any $t \geq 0$, the components of the controlled vector field (g_m, g_h) in (5) are smooth in the state variables (m, h). In addition, when $(m, h) \in [0, 1]^2$, we have that

$$\frac{\partial g_m}{\partial h} = A_m(1 - m) \geq 0 \ , \ \ \frac{\partial g_h}{\partial m} = A_h(1 - h) \geq 0 \ . \tag{35}$$

By Definition 10 right below, we deduce that the time-varying vector field — obtained from (g_m, g_h) in (5) with u replaced by $u(t)$ — is quasi monotonous in (m, h) for any $t \geq 0$.

Denote by $(\overline{g_m}, \overline{g_h})$ the vector field (g_m, g_h) in (5) when $u = \overline{u}$ in (5). Since $\overline{g_m} \leq g_m$ and $\overline{g_h} \leq g_h$, thanks to the comparison Theorem 12 we obtain the following the result: if $\overline{m}(0) \leq m(0)$ and $\overline{h}(0) \leq h(0)$, then $\overline{m}(t) \leq m(t)$ and $\overline{h}(t) \leq h(t)$, for every $t \geq 0$. □

Recalls on comparison theorems for differential systems

Definition 10. *The function $g : \mathbb{R}^n \to \mathbb{R}^n$ is said to be* quasi monotonous *if g is C^1 and that*

$$\frac{\partial g^i}{\partial x_j} \geq 0 \ , \ \ \forall i \neq j \ .$$

In what follows, all inequalities between vectors have to be understood componentwise.

Theorem 11. *Let f and g be two vector fields on $D \subset \mathbb{R}^n$, with f or g quasi monotonous and $f \leq g$. Suppose that the differential systems*

$$\dot{x} = f(x) \ , \ \ \dot{y} = g(y) \ ,$$

have solutions $t \mapsto x_t$ and $t \mapsto y_t$ defined for all $t \geq 0$. Then, if $x_0 \leq y_0$, we have that $x_t \leq y_t$ for all $t \geq 0$.

Proof. We consider two cases.

(a) Suppose that $f < g$ — that is, $f^i < g^i$ for all $i = 1, \ldots, n$ — and that $x_0 < y_0$. We define

$$\tau = \inf\{t \geq 0 \mid \exists i = 1, \ldots, n \ , \ \ x_t^i > y_t^i\} \ .$$

We show that $\tau = +\infty$, that is, $x_t \leq y_t$ for all $t \geq 0$. Indeed, let us suppose the contrary. If $\tau < +\infty$, then there exists at least one $i = 1, \ldots, n$ such that

$$x_\tau^i = y_\tau^i \ , \ \ x_\tau^j \leq y_\tau^j \ , \ \ \forall j \neq i \ .$$

Supposing that g is quasi monotonous (the proof is similar when f is quasi monotonous), we deduce that $g^i(x_\tau) \leq g^i(y_\tau)$.

Moreover, as $x_t^i > y_t^i$, for all $t \in]\tau, \tau+\epsilon[$ (for ϵ small enough) and $x_\tau^i = y_\tau^i$, we have that

$$f^i(x_\tau) = \frac{dx_t^i}{dt}_{|t=\tau} \geq \frac{dy_t^i}{dt}_{|t=\tau} = g^i(y_\tau) \ .$$

From $g^i(x_\tau) \leq g^i(y_\tau)$, $g^i(y_\tau) \leq f^i(x_\tau)$ and $f^i < g^i$, we deduce that

$$g^i(x_\tau) \leq g^i(y_\tau) \leq f^i(x_\tau) < g^i(x_\tau) \ .$$

This is contradictory. As a consequence, $x_0 < y_0$ implies that $x_t \leq y_t$ for all $t \geq 0$.

(b) Suppose that $f \leq g$ and $x_0 \leq y_0$. For any $\epsilon > 0$, denote by y_t^ϵ the solution of

$$\dot{y^\epsilon} = g(y^\epsilon) + \epsilon \ , \ \ y_0^\epsilon = y_0 + \epsilon \ .$$

We have that

$$x_0 < y_0^\epsilon \ , \ \ f < g + \epsilon \ .$$

Therefore, we can conclude from the previous item that $x_t \leq y_t^\epsilon$ for all $t \geq 0$. It is well known that, for fixed t, when $\epsilon \downarrow 0$, we have that $y_t^\epsilon \to y_t$.

As a consequence, $x_0 \leq y_0$ implies that $x_t \leq y_t$ for all $t \geq 0$.

□

The following extension is immediate.

Theorem 12. *Let $(f_t)_{t\geq 0}$ and $(g_t)_{t\geq 0}$ be two families of vector fields on $D \subset \mathbb{R}^n$, with f_t or g_t quasi monotonous and $f_t \leq g_t$, for all $t \geq 0$. Suppose that the differential systems*

$$\dot{x} = f_t(x) \ , \ \ \dot{y} = g_t(y) \ ,$$

have solutions $t \mapsto x_t$ and $t \mapsto y_t$ defined for all $t \geq 0$. Then, if $x_0 \leq y_0$, we have that $x_t \leq y_t$ for all $t \geq 0$.

B Appendix. Proof of Theorem 2

We have broken the proof of Theorem 2 into three subsections §B.2, §B.1 and §B.3.

C) Comfortable case. When the infection cap $\overline{H}$ is *high* as in (14), hence allowing the proportion of infected humans to be large in (10), the viability kernel is the entire constraint set $\mathbb{V}^0(\overline{H})$ in (12), as we will show in §B.1.

D) Desperate case. When the conditions (16) are met, strong state and control constraints are put and we will prove in §B.2 that the viability kernel (11) reduces to the origin $\{(0,0)\}$.

V) Viable case. Finally, when the conditions (18) are met — which is a more interesting case — the viability kernel (11) is a strict subset of the constraint set $\mathbb{V}^0(\overline{H})$ in (12), whose upper right frontier is a smooth curve that we characterize. The proof of this result will be given in §B.3.

Each subsection states a main Proposition, with its proof, possibly broken in Lemmas.

B.1 Comfortable case C)

When the imposed state constraints (10) are weak, meaning that the infection cap $\overline{H}$ on the proportion of infected humans is high as in (14), the viability kernel $\mathbb{V}(\overline{H},\overline{u})$ is the entire constraint set $\mathbb{V}^0(\overline{H})$ in (12) as follows.

Proposition 13. *If*

$$\frac{A_h}{A_h+\gamma} \leq \overline{H} \ , \tag{36}$$

the constraint set $\mathbb{V}^0(\overline{H})$ *in* (12) *is strongly invariant and is, therefore, the viability kernel:*

$$\mathbb{V}(\overline{H},\overline{u}) = \mathbb{V}^0(\overline{H}) = [0,1]\times[0,\overline{H}] \ . \tag{37}$$

Proof. Consider the controlled vector field (g_m, g_h) described in (5), which corresponds to the controlled dynamical system (4). We will study the vector (g_m, g_h) along the four faces of the rectangle $\mathbb{V}^0(\overline{H})$ and we will prove that, for any control, (g_m, g_h) is an inward-pointing vector, with respect to

the set $\mathbb{V}^0(\overline{H})$ (that is, the vector (g_m, g_h) belongs to the tangent cone, which is closed). Thanks to Proposition 7 (in fact, a time-varying extension), this suffices to prove that $\mathbb{V}^0(\overline{H})$ is strongly invariant.

- For any state (m, h) on the vertical half-line $m = 0$ and $h \geq 0$, we have that:

$$g_m(0, h, u) = A_m h \geq 0 \ , \ \ g_h(0, h) = -\gamma h \leq 0 \ . \tag{38}$$

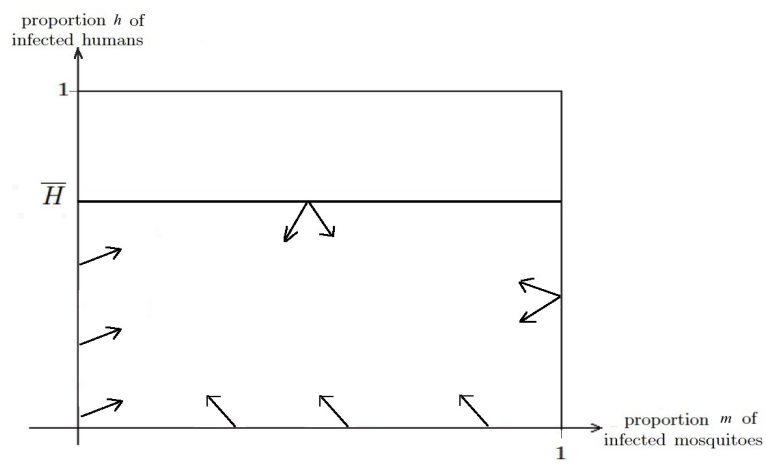

Figure 6: Controlled vector field (g_m, g_h) in (5) on the frontier of the constraint set $\mathbb{V}^0(\overline{H})$ in (12)

  Therefore, for any control $u \in [\underline{u}, \overline{u}]$, the vector (g_m, g_h) in (5) always points towards the inside of $\mathbb{V}^0(\overline{H})$ (see the left part of Figure 6).

- For any state (m, h) on the horizontal half-line $h = 0$ and $m \geq 0$, we have that:

$$g_m(m, 0, u) = -um \leq 0 \ , \ \ g_h(m, 0) = A_h m \geq 0 \ . \tag{39}$$

  Therefore, for any control $u \in [\underline{u}, \overline{u}]$, the vector (g_m, g_h) in (5) always points towards the inside of $\mathbb{V}^0(\overline{H})$ (see the bottom part of Figure 6).

- For any state (m, h) on the vertical line $m = 1$, we have that

$$g_m(1, h, u) = -u \leq -\underline{u} = -\delta \leq 0 \ , \tag{40}$$

since the natural mortality rate δ is nonnegative (see Table 1). Therefore, for any control $u \in [\underline{u}, \overline{u}]$, the vector (g_m, g_h) in (5) always points to the left of the line $m = 1$. Hence, the vector (g_m, g_h) always points towards the inside of $\mathbb{V}^0(\overline{H})$ (see the right part of Figure 6).

- Finally, for any state (m, h) on the horizontal half-line $h = \overline{H}$ and $m \leq 1$, we have that

$$g_h(m, \overline{H}) = A_h m(1 - \overline{H}) - \gamma \overline{H} \leq A_h(1 - \overline{H}) - \gamma \overline{H} \leq 0 \ , \tag{41}$$

by (36) (which is equivalent to $A_h(1 - \overline{H}) \leq \gamma \overline{H}$). Therefore, for any control $u \in [\underline{u}, \overline{u}]$, the vector (g_m, g_h) in (5) always points below the line $h = \overline{H}$. Hence, the vector (g_m, g_h) always points towards the inside of $\mathbb{V}^0(\overline{H})$ (see the top part of Figure 6).

Therefore, the constraint set $\mathbb{V}^0(\overline{H})$ is strongly invariant. So, the viability kernel $\mathbb{V}(\overline{H}, \overline{u})$ is $\mathbb{V}^0(\overline{H})$ because every trajectory of (6) that starts from $\mathbb{V}^0(\overline{H})$ remains in $\mathbb{V}^0(\overline{H})$, hence satisfies the state constraints (10). □

B.2 Desperate case D)

When both the control constraints (8) and the state constraints (10) are strong, the viability kernel (11) reduces to the origin $\{(0, 0)\}$ as follows.

Proposition 14. *If*

$$A_m(A_h + \gamma)\overline{H} + \gamma \overline{u} < A_m A_h \ , \tag{42}$$

the viability kernel (11) *only consists of the origin:*

$$\mathbb{V}(\overline{H}, \overline{u}) = \{(0, 0)\} \ . \tag{43}$$

Proof. First, note that the state $(0, 0)$ is a viable equilibrium, as seen in Proposition 4. Second, if the initial conditions $\big(m(0), h(0)\big)$ are taken outside $\{(0, 0)\}$, let us show that, for any admissible control trajectory $u(\cdot)$ the solution to (4) violates one of the state constraints (10).

Indeed, let $\overline{m}(t)$ and $\overline{h}(t)$ be solutions to (4) when $u(t) = \overline{u}$ and with initial state $\big(m(0), h(0)\big)$. The assumption (42), together with $\overline{H} > 0$ by (9), implies that $0 < A_h A_m - \gamma \overline{u}$. This is the condition (32) that makes the endemic equilibrium point

$$(m^e_{\overline{u}}, h^e_{\overline{u}}) = \left(\frac{A_m - \gamma \overline{u}/A_h}{A_m + \overline{u}}, \frac{A_h - \gamma \overline{u}/A_m}{A_h + \gamma} \right) \tag{44}$$

exist and display global asymptotic stability, as seen in Proposition 4. Hence, $\overline{h}(t)$ approaches $h^e_{\overline{u}}$ with $\overline{H} < h^e_{\overline{u}}$. So, by (42) and (44), we have $\overline{h}(t) > \overline{H}$ for all t large enough.

From Proposition 9, we have that $\overline{h}(t) \leq h(t)$, for every $t \geq 0$, so, for a sufficiently large t, we have that $\overline{H} < \overline{h}(t) \leq h(t)$.

Therefore, for any initial condition outside $\{(0,0)\}$, for any admissible control trajectory $u(\cdot)$, the solution to (4) violates the state constraints (10) for times t large enough, hence at least for one time. □

B.3 Viable case V)

When the control constraints (8) and the state constraints (10) are medium — that is, not too weak or too strong — the viability kernel $\mathbb{V}(\overline{H}, \overline{u})$ is in-between the origin $\{(0,0)\}$ and the entire constraint set $\mathbb{V}^0(\overline{H})$ in (12).

Proposition 15. *If*

$$\overline{H} < \frac{A_h}{A_h + \gamma} \ , \tag{45a}$$

$$A_m(A_h + \gamma)\overline{H} + \gamma\overline{u} > A_m A_h \ , \tag{45b}$$

we have that

- *the quantity $\overline{M}$, as defined in* (20) *is such that*

$$0 < \overline{M} < 1 \ , \tag{46}$$

- *the differential equation*

$$-g_m(m, \mathcal{H}(m), \overline{u})\mathcal{H}'(m) + g_h(m, \mathcal{H}(m)) = 0 \ , \tag{47a}$$

  with initial condition

$$\mathcal{H}(\overline{M}) = \overline{H} \ , \tag{47b}$$

  has a unique nonnegative solution $\mathcal{H}$,

- *this solution $\mathcal{H}$ is of the form*

$$\mathcal{H} : [\overline{M}, M_\infty] \to [0, \overline{H}] \ , \tag{48a}$$

with $M_\infty > \overline{M}$ *such that*

$$\begin{array}{rll} \textit{either} & \overline{M} < M_\infty < 1 & \textit{and } \mathcal{H}(M_\infty) = 0 \ , \qquad (48b) \\ \textit{or} & M_\infty = 1 & \textit{and } \mathcal{H}(M_\infty) > 0 \ , \qquad (48c) \end{array}$$

- *the viability kernel* (11) *is given by* $\mathbb{V}(\overline{H}, \overline{u}) =$

$$\big([0, \overline{M}] \times [0, \overline{H}]\big) \bigcup \Big\{ (m, h) \Big| \overline{M} \leq m \leq M_\infty \ , \ \ 0 \leq h \leq \mathcal{H}(m) \Big\} \ . \quad (49)$$

The proof consists of four lemmas. In Lemma 16, we describe the solution to (47a)–(47b) (Lemma 17 provides additional useful results). Lemma 18 shows that the set

$$\mathbb{V} = \big([0, \overline{M}] \times [0, \overline{H}]\big) \bigcup \Big\{ (m, h) \Big| \overline{M} \leq m \leq M_\infty \ , \ \ 0 \leq h \leq \mathcal{H}(m) \Big\} \quad (50)$$

is a viability domain for the controlled dynamical system (4), with the control constraints (8). Finally, in Lemma 19 we prove that the set $\mathbb{V}$, defined in (50), is the largest viability domain within the constraint set (12), hence is the viability kernel by Theorem 6.

Lemma 16. *When the inequalities* (45) *are fulfilled, there exists a function* $\mathcal{H}$*, solution to the differential equation* (47a) *which satisfies the initial condition* (47b) *and has the form* (48)*. The function* $\mathcal{H} : [\overline{M}, M_\infty] \to [\mathcal{H}(M_\infty), \overline{H}]$ *is a strictly decreasing one-to-one mapping.*

Proof. We conduct the proof in five steps.

1. First, we note that

$$\begin{aligned} g_m(\overline{M}, \overline{H}, \overline{u}) &= A_m \overline{H}(1 - \overline{M}) - \overline{u}\overline{M} \text{ by (5a)} \\ &= A_m \overline{H} - (A_m \overline{H} + \overline{u})\overline{M} \\ &= A_m \overline{H} - (A_m \overline{H} + \overline{u}) \frac{\gamma \overline{H}}{A_h(1 - \overline{H})} \text{ by definition (20) of } \overline{M} \\ &= \frac{\overline{H}}{A_h(1 - \overline{H})} [A_m A_h (1 - \overline{H}) - \gamma (A_m \overline{H} + \overline{u})] \\ &= \frac{\overline{H}}{A_h(1 - \overline{H})} [A_m A_h - \gamma \overline{u} - (A_m A_h + \gamma A_m) \overline{H}] \\ &< 0 \text{ by the left inequality of (45b).} \end{aligned}$$

By (5a), we easily deduce the following property, that will be useful later:[2]

$$m \geq \overline{M} \ , \ \ h \leq \overline{H} \Rightarrow g_m(m, h, \overline{u}) \leq g_m(\overline{M}, \overline{H}, \overline{u}) < 0 \ . \tag{51}$$

2. Second, we show that there is a local solution to the differential equation (47a)–(47b). Indeed, in the neighborhood of $(\overline{M}, \mathcal{H}(\overline{M})) = (\overline{M}, \overline{H})$, the coefficient $g_m(m, h, \overline{u})$ of $\mathcal{H}'(m)$ in (47a) is negative, as we just saw it in the previous item 1. Hence, in a neighborhood of $\overline{M}$, we can write (47a) as

$$\mathcal{H}'(m) = \frac{g_h(m, \mathcal{H}(m))}{g_m(m, \mathcal{H}(m), \overline{u})} = \frac{A_h m(1 - \mathcal{H}(m)) - \gamma \mathcal{H}(m)}{A_m \mathcal{H}(m)(1 - m) - \overline{u} m} \ . \tag{52}$$

Applying the Cauchy-Lipschitz theorem to (52)–(47b), we know that there exists a unique local C^1 solution $\mathcal{H}$ defined on an interval I around $\overline{M}$. We put

$$I_+ = I \cap [\overline{M}, +\infty[\ . \tag{53}$$

3. Third, we show that the local solution $\mathcal{H} : I_+ \to \mathbb{R}$ is strictly decreasing in the neighborhood of $\overline{M}$. For this purpose, we will study the sign of $g_h(m, \mathcal{H}(m))$ for $m \approx \overline{M}$. We have that

$$\begin{aligned} g_h(m, \mathcal{H}(m)) &= g_h(m, \mathcal{H}(m)) - g_h(\overline{M}, \overline{H}) \text{ by (22)} \\ &= A_h m(1 - \mathcal{H}(m)) - \gamma \mathcal{H}(m) - A_h \overline{M}(1 - \overline{H}) + \gamma \overline{H} \\ &= A_h(m - \overline{M})(1 - \overline{H}) + (A_h m + \gamma)(\overline{H} - \mathcal{H}(m)) \ . \end{aligned}$$

We have that $\mathcal{H}(m) - \overline{H} = o(m - \overline{M})$ when $m \to \overline{M}$. Indeed, the function $\mathcal{H}$ is C^1 and such that $\mathcal{H}'(\overline{M}) = 0$, by (52) since $g_h(\overline{M}, \overline{H}) = 0$ by (22). Therefore, we deduce that

$$g_h(m, \mathcal{H}(m)) = A_h(m - \overline{M})(1 - \overline{H}) + o(m - \overline{M}) \ . \tag{54}$$

Hence, when $m > \overline{M}$ and $m \approx \overline{M}$, we have that $g_h(m, \mathcal{H}(m)) > 0$. Therefore, by (52) and item 1, the function $\mathcal{H} : I_+ \to \mathbb{R}$ is strictly decreasing in a neighborhood of $\overline{M}$.

[2] If the left inequality of (45b) were not strict, we would have to consider the case $g_m(\overline{M}, \overline{H}, \overline{u}) = 0$. This would make the subsequent analysis more complicated. This is why we do not study the case $A_m(A_h + \gamma)\overline{H} + \gamma \overline{u} = A_m A_h$ in Theorem 2.

4. Fourth, we show that the local solution $\mathcal{H} : I_+ \to \mathbb{R}$ is strictly decreasing. Indeed, let us suppose the contrary: there exists $m \in I_+$, $m > \overline{M}$, such that $\mathcal{H}'(m) = 0$. We denote by $\tilde{m}$ the smallest of such m. By item 3, we know that $\mathcal{H}'(m) < 0$ in the neighborhood of $\overline{M}$ (except at $\overline{M}$), so that $\tilde{m} > \overline{M}$. By definition of $\tilde{m}$, we have that $\mathcal{H}'(m) < 0$ for $m \in]\overline{M}, \tilde{m}[$. Hence, $\mathcal{H}(\tilde{m}) < \mathcal{H}(\overline{M}) = \overline{H}$, so that

$$\begin{aligned} g_h(\tilde{m}, \mathcal{H}(\tilde{m})) &= A_h \tilde{m}(1 - \mathcal{H}(\tilde{m})) - \gamma \mathcal{H}(\tilde{m}) \text{ by (5)} \\ &> A_h \overline{M}(1 - \overline{H}) - \gamma \overline{H} \\ &= g_h(\overline{M}, \overline{H}) = 0 \text{ by (22)}. \end{aligned}$$

Therefore, $g_h(\tilde{m}, \mathcal{H}(\tilde{m})) > 0$. On the other hand, $g_m(\tilde{m}, \mathcal{H}(\tilde{m}), \overline{u}) < 0$ by the property (51), since $\tilde{m} > \overline{M}$ and $\mathcal{H}(\tilde{m}) < \overline{H}$. As a consequence, by the differential equation (52), we obtain that

$$\mathcal{H}'(\tilde{m}) = \frac{g_h(\tilde{m}, \mathcal{H}(\tilde{m}))}{g_m(\tilde{m}, \mathcal{H}(\tilde{m}), \overline{u})} < 0 \ .$$

We arrive at a contradiction, since $\mathcal{H}'(\tilde{m}) = 0$ by definition of $\tilde{m}$. Therefore, $\tilde{m}$ does not exist and the local solution $\mathcal{H} : I_+ \to \mathbb{R}$ is strictly decreasing.

5. Finally, we show that the local solution $\mathcal{H} : I_+ \to \mathbb{R}$ is such that (48) holds true. For this purpose, we consider two cases.

   - If, for every $m \in I_+$, $0 < \mathcal{H}(m)$, we show that $I_+ = [\overline{M}, +\infty[$. Indeed, as $\mathcal{H}$ decreases, we have $m \in I_+ \Rightarrow 0 < \mathcal{H}(m) \leq \mathcal{H}(\overline{M}) = \overline{H}$. Hence, we deduce that the solution $\mathcal{H}(m)$ to the equation (47a) exists over $m \in [\overline{M}, +\infty[$. We denote $M_\infty = 1$.
   - If there exists an $m \in I_+$ such that $\mathcal{H}(m) = 0$, we denote by $\tilde{m}$ the smallest of such m. We have that $\mathcal{H}(\tilde{m}) = 0$ and, since $\mathcal{H}$ decreases, we have that $\mathcal{H}(\tilde{m}) = 0 \leq \mathcal{H}(m) \leq \mathcal{H}(\overline{M}) = \overline{H}$ for every $m \in [\overline{M}, \tilde{m}]$.

     We consider two subcases, as illustrated in Figures 2 and 3.

     - If $\tilde{m} < 1$, we have that $\mathcal{H}(\tilde{m}) = 0$ and that $0 \leq \mathcal{H}(m) \leq \overline{H}$ for all $m \in [\overline{M}, \tilde{m}]$. We denote $M_\infty = \tilde{m} < 1$.
     - if $\tilde{m} \geq 1$, we deduce that $0 \leq \mathcal{H}(m) \leq \overline{H}$ for every $m \in [\overline{M}, 1]$. We denote $M_\infty = 1$.

Hence, we conclude that the solution to the differential equation (47a), which satisfies the initial condition (47b), is unique, has the form (48) and is strictly decreasing. As $\mathcal{H}(\overline{M}) = \overline{H}$, the function $\mathcal{H} : [\overline{M}, M_\infty] \to [\mathcal{H}(M_\infty), \overline{H}]$ is a strictly decreasing one-to-one mapping. $\square$

We know show that the curve generated by the solution $\mathcal{H}$ is an orbit.

Lemma 17. *The curve*

$$\{\big(m, \mathcal{H}(m)\big) \mid m \in [\overline{M}, M_\infty]\} \tag{55}$$

is an orbit of the controlled vector field (g_m, g_h) *in* (5)*, for the control* $\overline{u}$*. Indeed, for all*

$$\overline{\overline{m}}_0 \in [\overline{M}, M_\infty] \text{ and } \overline{\overline{h}}_0 = \mathcal{H}(\overline{\overline{m}}_0) \in [\mathcal{H}(M_\infty), \overline{H}] \ , \tag{56}$$

there exists $T \geq 0$ *such that the orbit of the trajectory* $t \in [0, T] \mapsto \big(\overline{\overline{m}}(t), \overline{\overline{h}}(t)\big)$ *— the solution to* (4) *when* $u(t) = \overline{u}$ *and when the starting point is* $\big(\overline{\overline{m}}(0), \overline{\overline{h}}(0)\big) = (\overline{\overline{m}}_0, \overline{\overline{h}}_0)$ *— is included in the curve* (55)*. In addition,*

$$\overline{\overline{m}}(T) = \overline{M} \text{ and } \overline{\overline{h}}(T) = \overline{H} \ . \tag{57}$$

Proof. When $\overline{\overline{m}}_0 = \overline{M}$, then $\mathcal{H}(\overline{\overline{m}}_0) = \mathcal{H}(\overline{M}) = \overline{H}$ by (47b), and the point $\big(\overline{\overline{m}}_0, \overline{\overline{h}}_0\big) = (\overline{M}, \overline{H})$ indeed belongs to the curve (55). Therefore $T = 0$.

Now, we suppose that $\overline{\overline{m}}_0 > \overline{M}$, so that $\mathcal{H}(\overline{\overline{m}}_0) < \overline{H}$ because $\mathcal{H}$ is strictly decreasing by Lemma 16. We define

$$T = \inf\{t \geq 0 \mid \overline{\overline{m}}(t) < \overline{M} \text{ or } \overline{\overline{h}}(t) > \overline{H}\} \ , \tag{58}$$

which is such that $T > 0$, since $\overline{\overline{m}}(0) = \overline{\overline{m}}_0 > \overline{M}$ and $\overline{\overline{h}}(0) = \mathcal{H}(\overline{\overline{m}}_0) < \overline{H}$.

We prove that $T < +\infty$. We consider two cases depending on whether there is a single equilibrium or not.

- If the condition (32) is not satisfied, the disease free equilibrium $(0, 0)$ is the only equilibrium of the controlled vector field (g_m, g_h) in (5), for the control $\overline{u}$. As $(0, 0)$ is globally asymptotically stable (see the proof of Proposition 4), we have that $\overline{\overline{m}}(t) \to 0$ when $t \to +\infty$. we deduce that there is a time t such that $\overline{\overline{m}}(t) < \overline{M}$. As a consequence, T as defined in (58) is finite: $T < +\infty$.

- If the condition (32) is satisfied, the endemic equilibrium point $(m^e_{\overline{u}}, h^e_{\overline{u}})$ in (44) exists (see the proof of Proposition 4). By definition of an equilibrium point for the controlled vector field (g_m, g_h) in (5) with control $\overline{u}$, we have that $g_m(m^e_{\overline{u}}, h^e_{\overline{u}}, \overline{u}) = 0$. Therefore, as the left hand side of inequality (45b) can be restated as $h^e_{\overline{u}} < \overline{H}$, we deduce that $m^e_{\overline{u}} < \overline{M}$, by (51). As seen in Proposition 4, the endemic equilibrium point (44) displays global asymptotic stability. Therefore, $\overline{\overline{m}}(t) \to m^e_{\overline{u}}$ when $t \to +\infty$. As $m^e_{\overline{u}} < \overline{M}$, we deduce that there is a time t such that $\overline{\overline{m}}(t) < \overline{M}$. As a consequence, T as defined in (58) is finite: $T < +\infty$.

We now study the trajectory $t \in [0, T] \mapsto \big(\overline{\overline{m}}(t), \overline{\overline{h}}(t)\big)$. By definition (58) of T, we have that

$$\overline{\overline{m}}(T) = \overline{M} \text{ or } \overline{\overline{h}}(T) = \overline{H} \ , \tag{59a}$$

and that

$$\overline{\overline{m}}(t) \geq \overline{M} \text{ and } \overline{\overline{h}}(t) \leq \overline{H} \ , \ \ \forall t \in [0, T] \ . \tag{59b}$$

By (51) and (59b), we deduce that

$$\frac{d\overline{\overline{m}}(t)}{dt} = g_m(\overline{\overline{m}}(t), \overline{\overline{h}}(t), \overline{u}) < 0 \ , \ \ \forall t \in [0, T] \ .$$

As $\overline{\overline{m}}_0 \leq M_\infty$ by (56), we deduce that $\overline{\overline{m}}(t) \leq \overline{\overline{m}}_0 \leq M_\infty$, for all $t \in [0, T]$. Together with $\overline{\overline{m}}(t) \geq \overline{M}$, we obtain that $\overline{\overline{m}}(t) \in [\overline{M}, M_\infty]$, for all $t \in [0, T]$. Therefore, $\mathcal{H}(\overline{\overline{m}}(t))$ is well defined since $\mathcal{H} : [\overline{M}, M_\infty] \to [\mathcal{H}(M_\infty), \overline{H}]$ by (48). We have, for all $t \in [0, T]$,

$$\begin{aligned}\frac{d}{dt}[\overline{\overline{h}}(t) - \mathcal{H}(\overline{\overline{m}}(t))] =& g_h(\overline{\overline{m}}(t), \overline{\overline{h}}(t)) - \mathcal{H}'(\overline{\overline{m}}(t)) g_m(\overline{\overline{m}}(t), \overline{\overline{h}}(t), \overline{u}) \\ & \text{by (4) and (5)} \\ =& 0 \text{ by (47a).}\end{aligned}$$

Therefore, for all $t \in [0, T]$,

$$\overline{\overline{h}}(t) - \mathcal{H}(\overline{\overline{m}}(t)) = \overline{\overline{h}}(0) - \mathcal{H}(\overline{\overline{m}}(0)) = 0 \text{ by (56)}, \tag{60}$$

so that the trajectory $t \in [0, T] \mapsto \big(\overline{\overline{m}}(t), \overline{\overline{h}}(t)\big)$ is included in the curve (55).

As a particular case, we have that $\overline{\overline{h}}(T) - \mathcal{H}(\overline{\overline{m}}(T)) = 0$. As $\overline{\overline{m}}(T) = \overline{M}$ or $\overline{\overline{h}}(T) = \overline{H}$ by (59a), we conclude that

$$\overline{\overline{m}}(T) = \overline{M} \text{ and } \overline{\overline{h}}(T) = \overline{H} \ ,$$

since the function $\mathcal{H} : [\overline{M}, M_\infty] \to [\mathcal{H}(M_\infty), \overline{H}]$ is a strictly decreasing one-to-one mapping. We have proven (57). □

Lemma 18. *When the inequalities* (45) *are fulfilled, the set* $\mathbb{V}$*, defined in* (50)*, is a viability domain for the controlled dynamical system* (4)*, with the control constraints* (8)*.*

Proof. Let the *Hamiltonian* $\mathcal{L}$ be defined, for every vector (n_m, n_h), every state (m, h) and control u, by

$$\mathcal{L}(m, h, n_m, n_h, u) = g_m(m, h, u)n_m + g_h(m, h)n_h \ . \tag{61}$$

The Hamiltonian is the scalar product between the vectors (g_m, g_h) in (5) and (n_m, n_h).

We will check that, for any given point along the piecewise-smooth frontier of the set $\mathbb{V}$, defined in (50), there is at least one control $u \in [\underline{u}, \overline{u}]$ such that the value (61) of the Hamiltonian is lower than or equal to zero when (n_m, n_h) is a normal outward-pointing vector (with respect to the set $\mathbb{V}$). For kink points between two smooth parts, we will do the same but with the cone generated by two normal outward-pointing vectors, corresponding to each of the smooth parts.

We will divide the frontier of the set $\mathbb{V}$, defined in (50), in five or seven parts (see Figures 2 and 3) as follows.

(a) On the horizontal segment $\{(m, 0)|0 < m < M_\infty\}$, on the vertical segment $\{(0, h)|0 < h < \overline{H}\}$ and at the points $(0, 0)$ and $(0, \overline{H})$, all vectors (g_m, g_h) in (5) point towards the inside of the set $\mathbb{V}$, defined in (50). Indeed, it suffices to copy the proof of Proposition 13.

(b) Along the segment $\{(m, \overline{H})|0 < m < \overline{M}\}$, a normal outward-pointing vector is

$$\begin{pmatrix} n_m \\ n_h \end{pmatrix} = \begin{pmatrix} 0 \\ 1 \end{pmatrix} \ .$$

Therefore, for any control $u \in [\underline{u}, \overline{u}]$, the value (61) of the Hamiltonian is

$$\mathcal{L}(m, \overline{H}, n_m, n_h, u) = g_h(m, \overline{H}) \times 1 < 0 \ ,$$

by (22) and because $m < \overline{M}$.

(c) Along the curve $\{(m, \mathcal{H}(m)) | \overline{M} < m < M_\infty\}$, a normal outward-pointing vector is

$$\begin{pmatrix} n_m \\ n_h \end{pmatrix} = \begin{pmatrix} -\mathcal{H}'(m) \\ 1 \end{pmatrix} \ .$$

Therefore, for the control $\overline{u}$, the value (61) of the Hamiltonian is

$$\mathcal{L}(m, \overline{H}, n_m, n_h, \overline{u}) = -g_m(m, \mathcal{H}(m), \overline{u})\mathcal{H}'(m) + g_h(m, \mathcal{H}(m)) \times 1 = 0 \ ,$$

because the function $\mathcal{H}$ is the solution to the differential equation (47a).

(d) The point $(\overline{M}, \overline{H})$ is a kink, to which is attached a cone of normal vectors generated by the two following normal outward-pointing vectors.

- A normal outward-pointing vector to the horizontal segment $\{(m, \overline{H}) | 0 \leq m \leq \overline{M}\}$ at the kink point $(\overline{M}, \overline{H})$ is

$$\begin{pmatrix} n_m \\ n_h \end{pmatrix} = \begin{pmatrix} 0 \\ 1 \end{pmatrix} \ .$$

  Therefore, for any control $u \in [\underline{u}, \overline{u}]$, the value (61) of the Hamiltonian is

$$\mathcal{L}(\overline{M}, \overline{H}, n_m, n_h, u) = g_h(\overline{M}, \overline{H}) \times 1 = 0 \text{ by (22).}$$

- A normal outward-pointing vector to the curve $\{(m, \mathcal{H}(m)) | \overline{M} \leq m \leq M_\infty\}$ at the kink point $(\overline{M}, \overline{H})$ is

$$\begin{pmatrix} n_m \\ n_h \end{pmatrix} = \begin{pmatrix} -\mathcal{H}'(M) \\ 1 \end{pmatrix} = \begin{pmatrix} 0 \\ 1 \end{pmatrix} \text{ by (52) and (22).}$$

  Therefore, for any control $u \in [\underline{u}, \overline{u}]$, the value (61) of the Hamiltonian is

$$\mathcal{L}(\overline{M}, \overline{H}, n_m, n_h, u) = g_h(\overline{M}, \overline{H}) \times 1 = 0 \text{ by (22).}$$

We conclude that, for any control $u \in [\underline{u}, \overline{u}]$, the value (61) of the Hamiltonian is zero for any combination of the two normal outward-pointing vectors above. As a consequence, all vectors (g_m, g_h) in (5) point towards the inside of the set $\mathbb{V}$, defined in (50), at the kink point $(\overline{M}, \overline{H})$.

(e) When $M_\infty < 1$ in (48) (see Figure 2), there only remains to consider the kink point $(M_\infty, 0)$.

- A normal outward-pointing vector to the horizontal segment $\{(m, 0) | 0 \leq m \leq M_\infty\}$ at the kink point $(M_\infty, 0)$ is

$$\begin{pmatrix} n_m \\ n_h \end{pmatrix} = \begin{pmatrix} 0 \\ -1 \end{pmatrix} .$$

  Therefore, for any control $u \in [\underline{u}, \overline{u}]$, the value (61) of the Hamiltonian is

$$\mathcal{L}(M_\infty, 0, n_m, n_h, u) = g_h(M_\infty, 0) \times (-1) = -A_h M_\infty < 0 .$$

- A normal outward-pointing vector to the curve $\{(m, \mathcal{H}(m)) | \overline{M} \leq m \leq M_\infty\}$ at the kink point $(M_\infty, 0)$ is

$$\begin{pmatrix} n_m \\ n_h \end{pmatrix} = \begin{pmatrix} -\mathcal{H}'(M_\infty) \\ 1 \end{pmatrix} .$$

  Therefore, for the control $\overline{u}$, the value (61) of the Hamiltonian is

$$\begin{aligned} \mathcal{L}(M_\infty, 0, n_m, n_h, \overline{u}) &= -g_m(M_\infty, 0, \overline{u})\mathcal{H}'(M_\infty) + g_h(M_\infty, 0) \times 1 \\ &= 0 \text{ by (47a).} \end{aligned}$$

We conclude that, for the control $\overline{u}$, the value (61) of the Hamiltonian is less than or equal to zero for any combination of the two normal outward-pointing vectors above. As a consequence, the vector (g_m, g_h) in (5), for the control $\overline{u}$, points towards the inside of the set $\mathbb{V}$, defined in (50), at the kink point $(M_\infty, 0)$.

(f) When $M_\infty = 1$ in (48) (see Figure 3), we have to consider the vertical segment $\{(1, h) | 0 \leq h < \mathcal{H}(1)\}$. A normal outward-pointing vector to the vertical segment $\{(1, h) | 0 \leq h < \mathcal{H}(1)\}$ has the form

$$\begin{pmatrix} n_m \\ n_h \end{pmatrix} = \begin{pmatrix} 1 \\ 0 \end{pmatrix} .$$

Therefore, for any control $u \in [\underline{u}, \overline{u}]$, the value (61) of the Hamiltonian is

$$\mathcal{L}(1, h, n_m, n_h, u) = g_m(1, h, u) \times 1 = -u \leq -\underline{u} \leq 0 \ .$$

As a consequence, all vectors (g_m, g_h) in (5) point towards the inside of the set $\mathbb{V}$, defined in (50), along the vertical segment $\{(1, h) | 0 \leq h < \mathcal{H}(1)\}$.

(g) When $M_\infty = 1$ in (48) (see Figure 3), there remains to consider the kink point $(1, \mathcal{H}(1))$.

- A normal outward-pointing vector to the vertical segment $\{(1, h) | 0 \leq h \leq \mathcal{H}(1)\}$ at the kink point $(1, \mathcal{H}(1))$ is

$$\begin{pmatrix} n_m \\ n_h \end{pmatrix} = \begin{pmatrix} 1 \\ 0 \end{pmatrix} \ .$$

  Therefore, for any control $u \in [\underline{u}, \overline{u}]$, the value (61) of the Hamiltonian is

$$\mathcal{L}(1, \mathcal{H}(1), n_m, n_h, u) = g_m(1, \mathcal{H}(1), u) \times 1 = -u \leq -\underline{u} < 0 \ .$$

- A normal outward-pointing vector to the curve $\{(m, \mathcal{H}(m)) | \overline{M} < m < M_\infty\}$ at the kink point $(1, \mathcal{H}(1))$ is

$$\begin{pmatrix} n_m \\ n_h \end{pmatrix} = \begin{pmatrix} -\mathcal{H}'(1) \\ 1 \end{pmatrix} \ .$$

  Therefore, for the control $\overline{u}$, the value (61) of the Hamiltonian is

$$\begin{aligned} \mathcal{L}(1, \mathcal{H}(1), n_m, n_h, \overline{u}) &= -g_m(1, \mathcal{H}(1), \overline{u})\mathcal{H}'(1) + g_h(1, \mathcal{H}(1)) \times 1 \\ &= 0 \text{ by (47a).} \end{aligned}$$

We conclude that, for the control $\overline{u}$, the value (61) of the Hamiltonian is zero for any combination of the two normal outward-pointing vectors above. As a consequence, the vector (g_m, g_h) in (5), for the control $\overline{u}$, points towards the inside of the set $\mathbb{V}$, defined in (50), at the kink point $(1, \mathcal{H}(1))$.

From Proposition 8, we can conclude that $\mathbb{V}$, defined in (50), is a viability domain for the controlled dynamical system (4), with the control constraints (8). □

Lemma 19. *When the inequalities* (45) *are fulfilled, the set* $\mathbb{V}$*, defined in* (50)*, is the largest viability domain for the controlled dynamical system* (4) *with the control constraints* (8)*, within the constraint set* (12)*.*

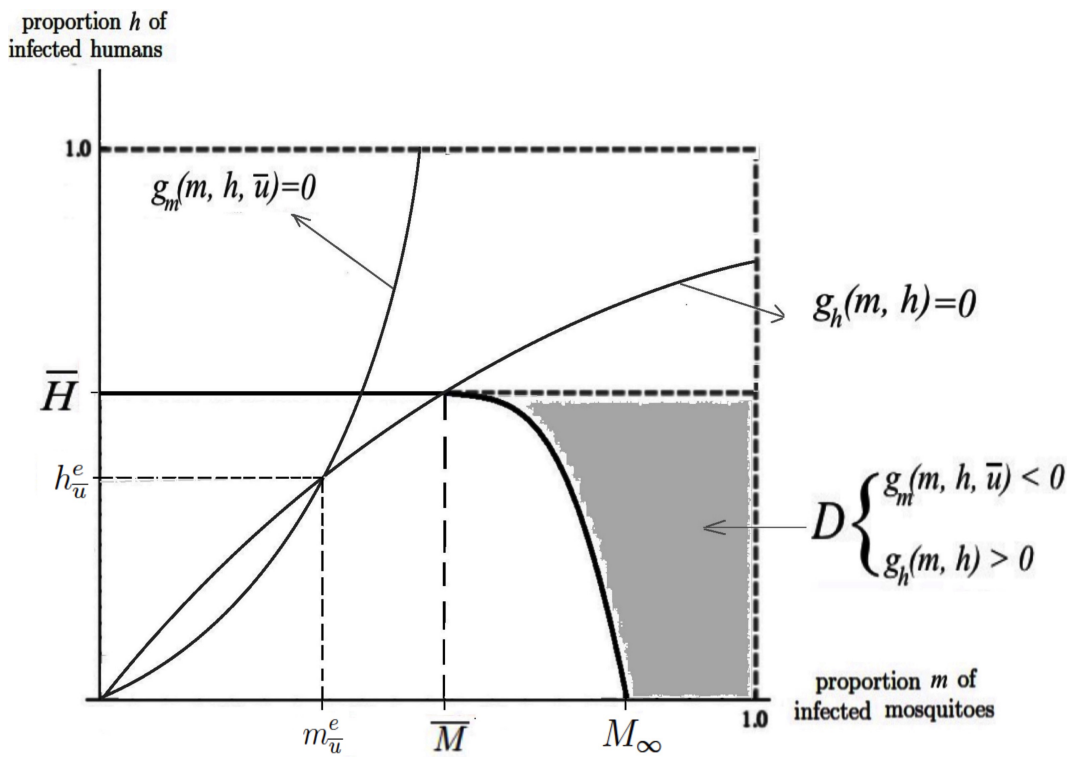

Figure 7: Phase portrait of the controlled vector field (g_m, g_h) in (5), with maximal control $u = \overline{u}$. The shaded portion corresponds to the complement of the viability kernel $\mathbb{V}(\overline{H}, \overline{u})$ with respect to the constraint set $\mathbb{V}^0(\overline{H})$, when $M_\infty < 1$

Proof. We prove that, for any control trajectory $u(\cdot)$ as in (8), the trajectory $t \mapsto \big(m(t), h(t)\big)$ solution of (4) and that starts from a point

$$\big(m(0), h(0)\big) = (m_0, h_0) \in \mathbb{V}^0(\overline{H})\backslash\mathbb{V} \tag{62}$$

does not satisfy one of the state constraints (10) for at least one $t > 0$. In Figure 7, the set $\mathbb{V}^0(\overline{H})\backslash\mathbb{V}$ is represented by the shaded part (in the case when $M_\infty < 1$).

First, we examine the point $(m_0, h_0) \in \mathbb{V}^0(\overline{H})\backslash\mathbb{V}$. On the one hand, as $(m_0, h_0) \in \mathbb{V}^0(\overline{H})$, we have that $0 \leq h_0 \leq \overline{H}$. On the other hand, since $(m_0, h_0) \notin \mathbb{V}$, where the set $\mathbb{V}$ is defined in (50), we deduce from Lemma 16, and especially from (48), that

$$(m_0, h_0) \in \mathbb{V}^0(\overline{H})\backslash\mathbb{V} \iff \overline{M} < m_0 \leq 1 \ , \ \ 0 \leq h_0 \leq \overline{H} \qquad (63)$$
$$\text{and} \begin{cases} \text{either} & m_0 > M_\infty \ , \\ \text{or} & m_0 \leq M_\infty \text{ and } \mathcal{H}(m_0) < h_0 \ . \end{cases}$$

Notice that, if $h_0 = \overline{H}$, then

$$\begin{aligned} \frac{dh(t)}{dt}_{|t=0} &= g_h(m_0, \overline{H}) \text{ by (4) and (5)} \\ &> g_h(\overline{M}, \overline{H}) \text{ by (5) and } \overline{M} < m_0 \\ &= 0 \text{ by (22).} \end{aligned}$$

Therefore, $h(t) > \overline{H}$, for $t > 0$ small enough. As a consequence, we will concentrate on the case $h_0 < \overline{H}$.

Second, we show that there exists a point $(\overline{\overline{m}}_0, \overline{\overline{h}}_0)$ such that

$$\overline{\overline{m}}_0 < m_0 \text{ and } \overline{\overline{m}}_0 \in [\overline{M}, M_\infty] \text{ and } \overline{\overline{h}}_0 = h_0 = \mathcal{H}(\overline{\overline{m}}_0) \leq \overline{H} \ . \qquad (64)$$

Of course, we take $\overline{\overline{h}}_0 = h_0$. To prove the existence of $\overline{\overline{m}}_0 \in [\overline{M}, M_\infty]$, it suffices to show that $h_0 \in [\mathcal{H}(M_\infty), \overline{H}]$. Indeed, we know from Lemma 16, and especially (48) that the function $\mathcal{H} : [\overline{M}, M_\infty] \to [\mathcal{H}(M_\infty), \overline{H}]$ is C^1 and strictly decreasing. Now, from (63), we deduce that

- if $M_\infty = 1$, then $m_0 \leq M_\infty = 1$ and $\mathcal{H}(m_0) < h_0 \leq \overline{H}$; as the function $\mathcal{H}$ is strictly decreasing, we conclude that $\mathcal{H}(M_\infty) \leq \mathcal{H}(m_0) < h_0 \leq \overline{H}$, hence that $h_0 \in [\mathcal{H}(M_\infty), \overline{H}]$;
- if $M_\infty < 1$, then $\mathcal{H}(M_\infty) = 0$ by (48); as $0 \leq h_0 \leq \overline{H}$, we conclude that $0 = \mathcal{H}(M_\infty) < h_0 \leq \overline{H}$, hence that $h_0 \in [\mathcal{H}(M_\infty), \overline{H}]$.

Notice in passing that, as the function $\mathcal{H}$ is strictly decreasing, we have that

$$\overline{\overline{m}}_0 = \overline{M} \iff \overline{\overline{h}}_0 = h_0 = \overline{H} \ . \qquad (65)$$

We have proved that $\overline{\overline{m}}_0$ exists and that $\overline{\overline{m}}_0 \in [\overline{M}, M_\infty]$. There remains to show that $\overline{\overline{m}}_0 < m_0$. Now, from $\overline{\overline{m}}_0 \in [\overline{M}, M_\infty]$ and $\overline{\overline{h}}_0 = h_0 = \mathcal{H}(\overline{\overline{m}}_0)$, we deduce that $(\overline{\overline{m}}_0, \overline{\overline{h}}_0) = (\overline{\overline{m}}_0, h_0) \in \mathbb{V}$, defined in (50). By definition (50) of $\mathbb{V}$, using the property that the function $\mathcal{H}$ is strictly decreasing, we have that

$$(\overline{\overline{m}}_0, \overline{\overline{h}}_0) = (\overline{\overline{m}}_0, h_0) \in \mathbb{V} \Rightarrow (m, h_0) \in \mathbb{V} \ , \ \ \forall m \leq \overline{\overline{m}}_0 \ .$$

As $(m_0, h_0) \notin \mathbb{V}$ by assumption (62), we conclude that $\overline{\overline{m}}_0 < m_0$.

From now on, we suppose that $h_0 < \overline{H}$, so that, summing up the properties shown above, the point $(\overline{\overline{m}}_0, \overline{\overline{h}}_0)$ is such that

$$\overline{\overline{m}}_0 < m_0 \text{ and } \overline{\overline{m}}_0 \in]\overline{M}, M_\infty] \text{ and } \overline{\overline{h}}_0 = h_0 = \mathcal{H}(\overline{\overline{m}}_0) < \overline{H} \ . \tag{66}$$

Now, in addition to the trajectory $t \mapsto \big(m(t), h(t)\big)$ that is the solution to (4) for the control trajectory $u(\cdot)$ when $\big(m(0), h(0)\big) = (m_0, h_0)$, we study the trajectories

- $t \mapsto \big(\overline{\overline{m}}(t), \overline{\overline{h}}(t)\big)$, the solution to (4) when $u(t) = \overline{u}$ and when the starting point is $\big(\overline{\overline{m}}(0), \overline{\overline{h}}(0)\big) = (\overline{\overline{m}}_0, \overline{\overline{h}}_0) = (\overline{\overline{m}}_0, h_0)$ as in (66), that is, on the right of the frontier of $\mathbb{V}$ (the bottom frontier of the shaded part in Figure 7);
- $t \mapsto \big(\overline{m}(t), \overline{h}(t)\big)$, the solution to (4) when $u(t) = \overline{u}$ and when the starting point is $\big(\overline{m}(0), \overline{h}(0)\big) = (m_0, h_0)$.

We have the following inequalities between initial conditions:

$$\big(\overline{\overline{m}}(0), \overline{\overline{h}}(0)\big) = (\overline{\overline{m}}_0, \overline{\overline{h}}_0) \leq (m_0, h_0) = \big(m(0), h(0)\big) = \big(\overline{m}(0), \overline{h}(0)\big) \ .$$

By Proposition 9, we deduce that

$$\big(\overline{\overline{m}}(t), \overline{\overline{h}}(t)\big) \leq \big(\overline{m}(t), \overline{h}(t)\big) \leq \big(m(t), h(t)\big) \ , \ \ \forall t \geq 0 \ .$$

By Lemma 17, we obtain in particular that there exists $T > 0$ such that

$$\overline{H} = \overline{\overline{h}}(T) \leq \overline{h}(T) \leq h(T) \ .$$

Here, $T > 0$ because (as can be seen in the proof of Lemma 17),

$$\overline{\overline{m}}(0) = \overline{\overline{m}}_0 > \overline{M} \text{ and } \overline{\overline{h}}(0) = \overline{\overline{h}}_0 < \overline{H} \ .$$

We prove that $\overline{\overline{h}}(T) < \overline{h}(T)$.

Suppose, by contradiction, that $\overline{\overline{h}}(T) = \overline{h}(T)$. Therefore, the function $t \geq 0 \mapsto \overline{h}(t) - \overline{\overline{h}}(t)$ is nonnegative with a minimum at $T > 0$, so that

$$\frac{d\overline{h}(t)}{dt}_{|t=T} - \frac{d\overline{\overline{h}}(t)}{dt}_{|t=T} = 0 \ .$$

From (4), we deduce that

$$A_h \overline{m}(T)(1 - \overline{h}(T)) - \gamma \overline{h}(T) = A_h \overline{\overline{m}}(T)(1 - \overline{\overline{h}}(T)) - \gamma \overline{\overline{h}}(T) \ .$$

As $\overline{\overline{h}}(T) = \overline{h}(T) < 1$, we obtain that $\overline{m}(T) = \overline{\overline{m}}(T)$. Therefore, we have

$$\big(\overline{\overline{m}}(T), \overline{\overline{h}}(T)\big) = \big(\overline{m}(T), \overline{h}(T)\big) \ .$$

This is impossible because the two trajectories $t \mapsto \big(\overline{\overline{m}}(t), \overline{\overline{h}}(t)\big)$, and $t \mapsto \big(\overline{m}(t), \overline{h}(t)\big)$ are generated by the same vector fields, so that they must be equal. However, we have $\overline{\overline{m}}(0) = \overline{\overline{m}}_0 < m_0 = \overline{m}(0)$.

To conclude, we have proven that, for any control trajectory $u(\cdot)$ as in (8), the state trajectory starting from any point of the set $\mathbb{V}^0(\overline{H}) \backslash \mathbb{V}$ does not satisfy one of the state constraints (10) for a time $T < +\infty$. $\square$

C Appendix. Epidemic model adjusted to the case of the dengue outbreak in 2013 in Cali, Colombia

The city of Cali, in Colombia, has witnessed several episodes of dengue, as displayed in Figure 8.

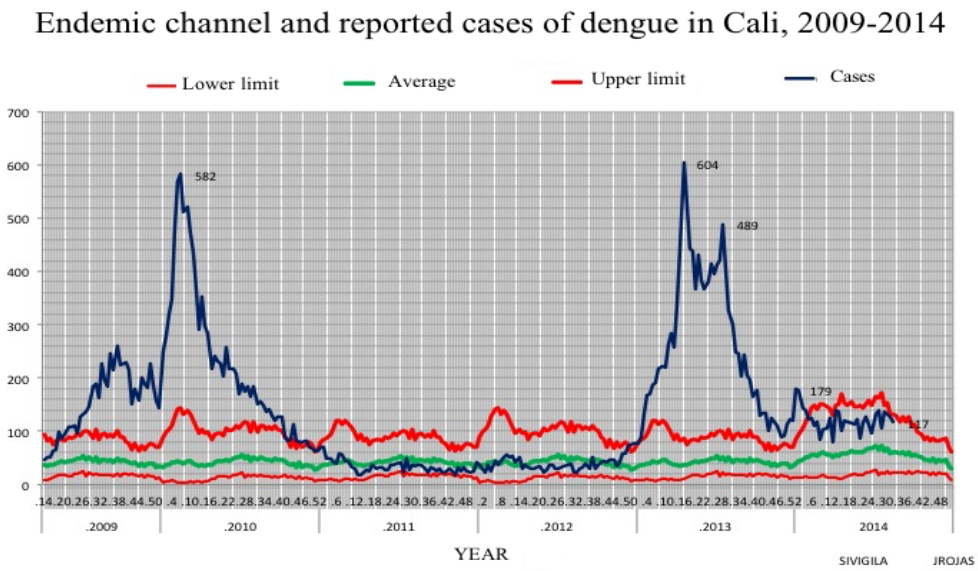

Figure 8: Number of infected by dengue, revealing several episodes of dengue in the city of Cali, in Colombia

The Municipal Secretariat of Public Health of Cali provided us with data corresponding to the dengue outbreak registered in 2013. Here, we present how we have estimated the parameters in the Ross-Macdonald model (1) — using the information of daily reports for new registered cases of dengue in Cali — to obtain different figures of viability kernels and of viable trajectories.

C.1 Parameters and daily data deduced from health reports

We introduce the vector of parameters

$$\theta = \big(\alpha, p_h, p_m, \xi, \delta\big) \in \Theta \subset \mathbb{R}^5_+ \ , \tag{67}$$

consisting of the five parameters previously defined in Table 1. The parameter set $\Theta \subset \mathbb{R}^5_+$ is given by the Cartesian product of the five intervals in the third column of Table 2.

With these notations, the Ross-Macdonald model (1) now writes

$$\begin{aligned} \frac{dm(t;\theta)}{dt} &= \alpha p_m h(t;\theta)\big(1 - m(t;\theta)\big) - \delta m \ , \\ \frac{dh(t;\theta)}{dt} &= \alpha p_h \xi m(t;\theta)\big(1 - h(t;\theta)\big) - \gamma h \ , \\ \big(m(0;\theta), h(0;\theta)\big) &= (m_0, h_0) \ . \end{aligned} \tag{68}$$

Notice that the rate γ of human recovery does not appear in the parameter vector θ in (67). Indeed, in the data we only have new cases of dengue registered per day; there is no information regarding how many inviduals recover daily. We choose an infectiousness period of 10 days, that is, a rate of human recovery fixed at

$$\gamma = 0.1 \text{ day}^{-1} \ . \tag{69}$$

Under this assumption, the *daily incidence data* (i.e., numbers of newly registered cases reported on daily basis) provided by the Municipal Secretariat of Public Health (Cali, Colombia) can be converted into the *daily prevalence data* (i.e., numbers of infected inviduals on a given day, be they new or not). With this, we deduce values of daily proportion of infected inviduals in the form of the set

$$\mathbb{O} = \Big\{ \big(t_j, \widehat{h}_j\big) \ , \ \ j = 0, 1, \ldots, \mathcal{D} \Big\} \ , \tag{70}$$

where t_j refers to j-th day, within the observation period of $(\mathcal{D}+1)$ days, and where $\widehat{h}_j$ stands for the fraction of infected inviduals at the day t_j. Naturally, the first couple in the set $\mathbb{O}$ in (70) defines the initial condition $h(0;\theta) = \widehat{h}_0$ (with $t_0 = 0$ the initial observation day). Unfortunately, there is no available data for the fraction of infected mosquitoes. As mosquito abundance is strongly correlated with dengue outbreaks [21], we have chosen a linear relation $m(0;\theta) = 3\widehat{h}_0$ at the beginning of an epidemic outburst (other choices gave similar numerical results).

C.2 Parameter estimation

To estimate a parameter vector $\theta \in \Theta$ that fits with the data, we apply the curve-fitting approach based on least-square method. More precisely, we look

for an optimal solution to the problem of constrained optimization

$$\min_{\theta\in\Theta}\sum_{j=1}^{\mathcal{D}}\left(h(t_j;\theta)-\widehat{h}_j\right)^2\ ,\ \ \mathcal{D}=60\text{ days}\ , \tag{71}$$

subject to the differential constraint (68). Regarding numerics, we have solved this optimization problem with the `lsqcurvefit` routine (MATLAB Optimization Toolbox), starting with an admissible $\theta_0 \in \Theta$ (see its exact value in Table 2, second column). The routine generates a sequence $\theta_1, \theta_2 \ldots$ that we stop once it is stationary, up to numerical precision. For a better result, we have combined two particular methods (Trust-Region-Reflective Least Squares Algorithm [30] and Levenberg-Marquardt Algorithm [25]) in the implementation of the `lsqcurvefit` MATLAB routine.

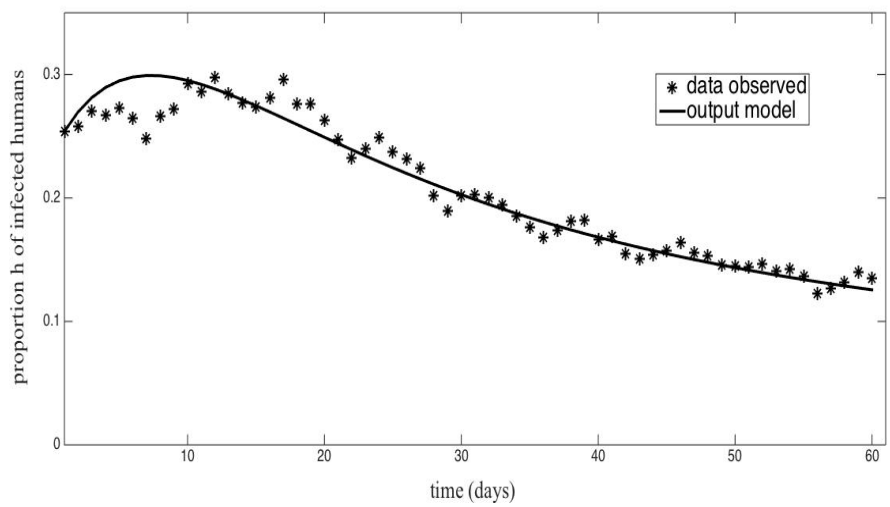

Figure 9: Fraction of inviduals infected with dengue, obtained by adjustment of the Ross-Macdonald model (1) (smooth solid curve) versus registered daily prevalence cases (star isolated points) during the 2013 dengue outbreak in Cali, Colombia

The last column of Table 2 provides estimated values for the parameters $\theta = \left(\alpha, p_h, p_m, \xi, \delta\right)$, and Figure 9 displays the curve-fitting results. Therefore, the aggregate parameters (2) and rate γ of human recovery are

Parameter	Initial value	Range	Reference	Estimated value	Unit
α	1	$[0, 5]$	[11], [27]	0.3600	day^{-1}
p_m	0.5	$[0, 1]$		0.2128	dimensionless
p_h	0.5	$[0, 1]$		0.1990	dimensionless
ξ	1	$[1, 5]$	[24], [28]	1.0087	dimensionless
δ	0.035	$[0.033, 0.066]$	[11], [28]	0.0333	day^{-1}

Table 2: Initial values, admissible ranges, respective source references, estimated values of parameters (numerical solution of the optimization problem (71)–(68)) and units

estimated as

$$A_m = 0.076608 \text{ day}^{-1} \ , \ \ A_h = 0.0722633 \text{ day}^{-1} \ , \ \ \gamma = 0.1 \text{ day}^{-1} \ . \tag{72a}$$

For the natural mortality rate $\delta = \underline{u}$ of mosquitoes (see Table 1), we obtain

$$\delta = \underline{u} = 0.0333 \text{ day}^{-1} \ . \tag{72b}$$

For the mosquito mortality maximal rate $\overline{u}$, we take

$$\overline{u} = 0.05 \text{ day}^{-1} \ . \tag{72c}$$

Acknowledgments. The authors thank the French program PEERS-AIRD (*Modèles d'optimisation et de viabilité en écologie et en économie*) and the Colombian Programa Nacional de Ciencias Básicas COLCIENCIAS (*Modelos y métodos matemáticos para el control y vigilancia del dengue*, código 125956933846) that offered financial support for missions, together with École des Ponts ParisTech (France), Université Paris-Est (France), Universidad Autónoma de Occidente (Cali, Colombia) and Universidad del Valle (Cali, Colombia). The authors thank the Handling editor and the three Reviewers for their helpful comments.

References

[1] R. M. Anderson and R. M. May. *Infectious Diseases of Humans: Dynamics and Control.* Oxford Science Publications. OUP Oxford, 1992.

[2] J. P. Aubin. *Viability theory*. Systems & Control: Foundations & Applications. Birkhäuser Boston Inc., Boston, MA, 1991.

[3] C. Béné, L. Doyen, and D. Gabay. A viability analysis for a bio-economic model. *Ecological Economics*, 36:385–396, 2001.

[4] D. Bertsekas and I. Rhodes. On the minimax reachability of target sets and target tubes. *Automatica*, 7:233–247, 1971.

[5] G. Bitsoris. On the positive invariance of polyhedral sets for discrete-time systems. *Systems and Control Letters*, 11(3):243–248, 1988.

[6] F. Blanchini. Set invariance in control (survey paper). *Automatica*, 35(11):1747–1767, 1999.

[7] N. Bonneuil and K. Müllers. Viable populations in a prey-predator system. *Journal of Mathematical Biology*, 35(3):261–293, February 1997.

[8] N. Bonneuil and P. Saint-Pierre. Population viability in three trophic-level food chains. *Applied Mathematics and Computation*, 169(2):1086 – 1105, 2005.

[9] F. Brauer and C. Castillo-Chávez. *Mathematical models in population biology and epidemiology*, volume 40 of *Texts in Applied Mathematics*. Springer-Verlag, New York, 2001.

[10] F. H. Clarke, Y. S. Ledayev, R. J. Stern, and P. R. Wolenski. Qualitative properties of trajectories of control systems: a survey. *Journal of Dynamical Control Systems*, 1:1–48, 1995.

[11] A. Costero, J. D. Edman, G. G. Clark, and T. W. Scott. Life table study of *Aedes aegypti* (diptera: Culicidae) in Puerto Rico fed only human blood plus sugar. *Journal of Medical Entomology*, 35(5):809–813, 1998.

[12] R. V. Culshaw, S. Ruan, and R. J. Spiteri. Optimal HIV treatment by maximising immune response. *Journal of Mathematical Biology*, 48(5):545–562, 2004.

[13] M. De Lara and L. Doyen. *Sustainable Management of Natural Resources. Mathematical Models and Methods*. Springer-Verlag, Berlin, 2008.

[14] O. Diekmann and J. A. P. Heesterbeek. *Mathematical Epidemiology of Infectious Diseases*. Wiley, Utrecht, Netherland, 2000.

[15] E. G. Gilbert and K. T. Tan. Linear systems with state and control constraints: the theory and application of maximal output admissible sets. *IEEE Transactions on Automatic Control*, 36(9):1008–1020, 1991.

[16] P.-O. Gutman and M. Cwikel. Admissible sets and feedback control for discrete-time linear dynamical systems with bounded controls and states. *IEEE Transactions on Automatic Control*, 31(4):373– 376, 1986.

[17] E. Hansen and T. Day. Optimal control of epidemics with limited resources. *Journal of Mathematical Biology*, pages 1–29, 2010.

[18] H. W. Hethcote. Optimal ages of vaccination for measles. *Mathematical Biosciences*, 89(1):29 – 52, 1988.

[19] H. W. Hethcote. The mathematics of infectious diseases. *SIAM Review*, 42:599–653, 2000.

[20] H. W. Hethcote and P. Waltman. Optimal vaccination schedules in a deterministic epidemic model. *Mathematical Biosciences*, 18(3-4):365 – 381, 1973.

[21] C. C. Jansen and N. W. Beebe. The dengue vector *Aedes aegypti*: what comes next. *Microbes and infection*, 12(4):272–279, 2010.

[22] D. Kirschner, S. Lenhart, and S. Serbin. Optimal control of the chemotherapy of HIV. *Journal of Mathematical Biology*, 35(7):775–792, 1997.

[23] I. M. Longini Jr, E. Ackerman, and L. R. Elveback. An optimization model for influenza A epidemics. *Mathematical Biosciences*, 38(1-2):141 – 157, 1978.

[24] F. Méndez, M. Barreto, J. F. Arias, G. Rengifo, J. Muñoz, M. E. Burbano, and B. Parra. Human and mosquito infections by dengue viruses during and after epidemics in a dengue-endemic region of Colombia. *Am J Trop Med Hyg.*, 74(4):678–683, 2006.

[25] J. J. Moré. The Levenberg-Marquardt algorithm: implementation and theory. In *Numerical analysis*, pages 105–116. Springer, 1978.

[26] L. Santacoloma, B. Chavez, and H. L. Brochero. Estado de la susceptibilidad de poblaciones naturales del vector del dengue a insecticidas en trece localidades de Colombia. *Biomédica*, 32(3):333–343, 2012.

[27] T. W. Scott, P. Amerasinghe, A. C. Morrison, L. H. Lorenz, G. G. Clark, D. Strickman, P. Kittayapong, and J. D. Edman. Longitudinal studies of *Aedes aegypti* (Diptera: Culicidae) in Thailand and Puerto Rico: blood feeding frequency. *Journal of medical entomology*, 37(1):89–101, 2000.

[28] T. W. Scott, A. C. Morrison, L. H. Lorenz, G. G. Clark, D. Strickman, P. Kittayapong, H. Zhou, and J. D. Edman. Longitudinal studies of *Aedes aegypti* (Diptera: Culicidae) in Thailand and Puerto Rico: population dynamics. *Journal of medical entomology*, 37(1):77–88, 2000.

[29] D. L. Smith, F. E. McKenzie, R. W. Snow, and S. I. Hay. Revisiting the basic reproductive number for malaria and its implications for malaria control. *PLoS Biol*, 5(3):e42, 02 2007.

[30] D. C. Sorensen. Newton's method with a model trust region modification. *SIAM Journal on Numerical Analysis*, 19(2):409–426, 1982.

[31] W. Walter. *Ordinary Differential Equations*. Graduate Texts in Mathematics. Springer New York, 1998.